

Practical Efficient Global Optimization is No-regret

Jingyi Wang

Lawrence Livermore National Laboratory, CA, USA

Haowei Wang

National University of Singapore, Singapore

Nai-Yuan Chiang

Lawrence Livermore National Laboratory, CA, USA

Juliane Mueller

National Laboratory of the Rockies, CO, USA

Tucker Hartland

Lawrence Livermore National Laboratory, CA, USA

Cosmin G. Petra

Lawrence Livermore National Laboratory, CA, USA

Abstract

Efficient global optimization (EGO) is one of the most widely used noise-free Bayesian optimization algorithms. It comprises the Gaussian process (GP) surrogate model and expected improvement (EI) acquisition function. In practice, when EGO is applied, a scalar matrix of a small positive value (also called a nugget or jitter) is usually added to the covariance matrix of the deterministic GP to improve numerical stability. We refer to this EGO with a positive nugget as the practical EGO. Despite its wide adoption and empirical success, to date, cumulative regret bounds for practical EGO have yet to be established. In this paper, we present for the first time the cumulative regret upper bound of practical EGO. In particular, we show that practical EGO has sublinear cumulative regret bounds and thus is a no-regret algorithm for commonly used kernels including the squared exponential (SE) and Matérn kernels ($\nu > \frac{1}{2}$). Moreover, we analyze the effect of the nugget on the regret bound and discuss the theoretical implication on its choice. Numerical experiments are conducted to support and validate our findings.

1 Introduction

Efficient global optimization (EGO) is a derivative-free optimization method that uses Gaussian process (GP) surrogate models to approximate and guide the optimization of black-box functions [22, 26, 49]. Given no observation noise, it is equivalent to Bayesian optimization (BO) with the expected improvement (EI) acquisition function. EGO has seen enormous success in many applications including machine learning [53], robotics [8], aerodynamic optimization design [21], etc, and has been extended to constrained BO [13], com-

binatorial problems [54], and multiple surrogates [47]. In the classic form, EGO aims to solve the optimization problem

$$\underset{\mathbf{x} \in C}{\text{minimize}} \quad f(\mathbf{x}), \quad (1)$$

where $\mathbf{x} \in \mathbb{R}^d$ is the decision variable, $C \subset \mathbb{R}^d$ represents the bound constraints on \mathbf{x} , and $f : \mathbb{R}^d \rightarrow \mathbb{R}$ is the black-box objective function.

EGO iteratively selects the candidate sample for the next observation using the EI acquisition function [23, 40]. EI computes the conditional expectation of an improvement function leveraging both the posterior mean and variance of the GP in search of the next sample. With a closed form, EGO is simple to implement and only requires the cumulative distribution function (CDF) and probability density function (PDF) of the standard normal distribution.

In practice, adding a small positive value, called a *nugget* or a *jitter* [12, 17], to the diagonal of the GP covariance matrix in EGO is often beneficial or even necessary [3] (see Section 2.1 for details). We denote the nugget as $\epsilon > 0$ in this paper. One of the main motivations for using ϵ is to improve the numerical stability of computations involving the inverse of the covariance matrix, *e.g.*, calculating posterior mean and variance. The covariance matrix is known to cause numerical issues due to ill-conditioning, which can occur when sample points are too close to each other [23]. Cholesky decomposition, which is invariably used to solve linear systems involving the covariance matrix, is known to break in finite-precision arithmetic for ill-conditioned matrices since very small (both positive and negative) pivots occur due to round-off errors [18, 24, 27, 30, 42, 51]. This numerical instability has long been recognized by the numerical optimization community and thoroughly investigated by proposing modified Cholesky decompositions employing positive semi-definite perturbations [14, 15, 39, 52], or positive

diagonal regularization terms [16], to circumvent the factorization breakdown.

Indeed, the use of ϵ is widely adopted in some of the most popular BO/EGO software packages. In the Surrogate Modeling Toolbox (SMT) [38], the EGO implementation with the GP (KRG) model uses a fixed $\epsilon = 2.220 \times 10^{-14}$ with the option of larger values. In Pyro [4], the GP regression model (GPModel) employs $\epsilon = 10^{-6}$ for stabilization of the Cholesky decomposition. In scikit-learn [33], the GP model (GPR) for EGO uses a default $\epsilon = 10^{-10}$. In Botorch [3], which uses GPyTorch [12], examples on GP regression models (SingleTaskGP) with noise-free observations are presented with $\epsilon = 10^{-6}$. GPyOpt [43] uses a trial-and-error approach, where $\epsilon = 10^{-10}$ is added when the Cholesky decomposition of the covariance matrix fails. BayesOpt [29], which is used in MATLAB, similarly raises errors when the Cholesky decomposition fails. Finally, we mention that in GPyTorch [12, 48], a positive nugget is instrumental in the well-posedness and efficiency of the proposed preconditioned batched conjugate gradient algorithm.

Apart from improving numerical stability, in recent years, the adoption of ϵ for deterministic GP fitting and EGO has been recommended for improved statistical properties. In [2], the authors studied the effect of the nugget and showed that by choosing appropriate values for ϵ and the length-scale hyper-parameter of the squared exponential (SE) kernel, the approximation errors of the GP can be arbitrarily small. In [17], the authors proposed adding ϵ in deterministic GP models for noise-free observations. They noted that its inclusion provided improved statistical properties of the GP model for many common scenarios. Similarly, [34] recommended using ϵ for noise-free observations. The authors claimed that the maximum likelihood estimate of the correlation parameter is more reliable and the condition number of the covariance matrix is moderate. In [5], the authors developed an adaptive strategy for choosing ϵ to improve the accuracy and efficiency in fitting the hyper-parameters of a GP model. Given its wide adoption in both literature and practical code implementation, we refer to EGO with a nugget $\epsilon > 0$ as the “*practical EGO*” in this paper.

While the *simple regret* bound of EGO has been studied in [7] in the frequentist setting, where f lies in a reproducing kernel Hilbert space (RKHS), existing works on the *cumulative regret* behavior of either EGO or practical EGO have clear limitations. Given t samples $\mathbf{x}_1, \dots, \mathbf{x}_t$, simple regret measures the error between the smallest observed function value and the optimal function value, *i.e.*, $f_t^+ - f^*$, where $f_t^+ = \min_{i=1, \dots, t} f(\mathbf{x}_i)$ and $f^* = \min_{\mathbf{x} \in C} f(\mathbf{x})$. On the other

hand, cumulative regret, denoted as R_T for T samples, measures the overall performance of the algorithm throughout the optimization process (see (9) for definition), and is the preferred metric in the multi-armed bandit paradigm [1, 25, 36] and many real-world applications [6]. It is desirable for an algorithm to have a sublinear R_T asymptotically, *i.e.*, $\lim_{T \rightarrow \infty} R_T/T = 0$. This property is called the no-regret property. Following the seminal work of [41], the cumulative regret bounds for some BO algorithms such as the upper confidence bound (UCB) and Thompson sampling (TS) have been studied extensively, including in the noise-free case [9, 28, 45].

However, the cumulative regret upper bounds for either EGO or practical EGO have not been established, despite EI being one of the most popular acquisition functions [11]. From a technical perspective, this is partially due to the inclusion of an incumbent in EI and its non-convex nonlinear nature [19, 37]. Existing works often make noticeable modifications to the EI acquisition function by introducing new hyper-parameters in order to achieve sublinear cumulative regret bounds. In [50], the authors studied a modified EI function with additional hyper-parameters and the best posterior mean incumbent. They further used the lower and upper bounds of the hyper-parameters to prove a sublinear cumulative regret bound. Similarly, [19] introduced an evaluation cost and modified EI. In [44], the authors also modified the EI by including additional control parameter and showed an upper bound for the sum of simple regret, not the cumulative regret. In [32], the authors added an additional stopping criterion to bound the instantaneous regret. However, it is unclear whether the stopping criterion guarantees an optimal solution upon exit.

The lack of cumulative regret analysis despite the empirical success of practical EGO leaves two important open questions: *Is practical EGO a no-regret algorithm? How does the nugget value affect regret behavior?* In this paper, we provide an affirmative answer to the first question and guidance to the second question by developing novel theoretical techniques. Our theoretical results can be used to explain and validate the empirical success of practical EGO. Our contributions in this paper are two-fold.

- First, we establish for the first time a cumulative regret upper bound $\mathcal{O}(\log^{1/2}(T)T^{1/2}\sqrt{\gamma_T})$ for practical EGO, one of the most widely used noise-free BO algorithms, where γ_T is the maximum information gain (Definition A.3). Thus, we prove that practical EGO is a no-regret algorithm for different kernels, as long as the γ_T of a kernel is sublinear. Specifically, the cumulative regret bounds are $\mathcal{O}(T^{1/2} \log^{(d+2)/2}(T))$ and

$\mathcal{O}(T^{\frac{\nu+d}{2\nu+d}} \log^{\frac{2\nu+0.5d}{2\nu+d}}(T))$ for SE and Matérn kernels, respectively (see (3) for definitions).

- Second, we study the effect of the nugget ϵ on practical EGO and its cumulative regret bounds, and thereby providing insight into the choice of ϵ .

This paper is organized as follows. In Section 2, we introduce GP, EI, practical EGO, and other necessary background information. In Section 3, we present the regret bound analysis starting with preliminary results in Section 3.1. In Section 3.2, the novel instantaneous regret bound is established. The cumulative regret bound is provided in Section 3.3. Limitation on extending the regret bound analysis to EGO is also presented at the end of Section 3. We discuss the effect of ϵ in Section 4. Numerical experiments are used to validate our findings in Section 5. Conclusions are made in Section 6.

2 Background

In this section, we first provide the basics of GPs and the EI acquisition function. Then, other backgrounds relevant to cumulative regret analysis are introduced.

2.1 Gaussian Process

Consider a zero mean GP with the kernel (*i.e.*, covariance function) $k(\mathbf{x}, \mathbf{x}') : \mathbb{R}^d \times \mathbb{R}^d \rightarrow \mathbb{R}$. Given the t th sample $\mathbf{x}_t \in C$, the observed function value is $f(\mathbf{x}_t)$. The $t \times t$ covariance matrix is denoted as $\mathbf{K}_t = [k(\mathbf{x}_1, \mathbf{x}_1), \dots, k(\mathbf{x}_1, \mathbf{x}_t); \dots; k(\mathbf{x}_t, \mathbf{x}_1), \dots, k(\mathbf{x}_t, \mathbf{x}_t)]$. The noise-free observations is $\mathbf{f}_{1:t} = [f(\mathbf{x}_1), \dots, f(\mathbf{x}_t)]^T$. Without the nugget ϵ , the posterior mean, denoted as μ_t^0 , and standard deviation, denoted as σ_t^0 , of the deterministic GP used in EGO is

$$\begin{aligned} \mu_t^0(\mathbf{x}) &= \mathbf{k}_t(\mathbf{x}) \mathbf{K}_t^{-1} \mathbf{f}_{1:t} \\ (\sigma_t^0(\mathbf{x}))^2 &= k(\mathbf{x}, \mathbf{x}) - \mathbf{k}_t(\mathbf{x})^T \mathbf{K}_t^{-1} \mathbf{k}_t(\mathbf{x}), \end{aligned}$$

where $\mathbf{k}_t(\mathbf{x}) = [k(\mathbf{x}_1, \mathbf{x}), \dots, k(\mathbf{x}_t, \mathbf{x})]^T$. Accounting for $\epsilon > 0$ and its corresponding scalar matrix $\epsilon \mathbf{I}$, the posterior mean μ_t and variance σ_t^2 used in practical EGO are

$$\begin{aligned} \mu_t(\mathbf{x}) &= \mathbf{k}_t(\mathbf{x}) (\mathbf{K}_t + \epsilon \mathbf{I})^{-1} \mathbf{f}_{1:t} \\ \sigma_t^2(\mathbf{x}) &= k(\mathbf{x}, \mathbf{x}) - \mathbf{k}_t(\mathbf{x})^T (\mathbf{K}_t + \epsilon \mathbf{I})^{-1} \mathbf{k}_t(\mathbf{x}), \end{aligned} \quad (2)$$

We emphasize that the observations $\mathbf{f}_{1:t}$ are noise-free in (2).

SE and Matérn kernels are among the most popular kernels for BO and GP. Their definitions are as follows.

$$\begin{aligned} k_{SE}(\mathbf{x}, \mathbf{x}') &= \exp\left(-\frac{r^2}{2l^2}\right), \\ k_{Matérn}(\mathbf{x}, \mathbf{x}') &= \frac{1}{\Gamma(\nu)2^{\nu-1}} \left(\frac{\sqrt{2\nu}r}{l}\right)^\nu B_\nu\left(\frac{\sqrt{2\nu}r}{l}\right). \end{aligned} \quad (3)$$

where $l > 0$ is the length hyper-parameter, $r = \|\mathbf{x} - \mathbf{x}'\|_2$, $\nu > 0$ is the smoothness parameter of the Matérn kernel, and B_ν is the modified Bessel function of the second kind.

2.2 Expected Improvement

The improvement function of f given t samples is defined as

$$I_t(\mathbf{x}) = \max\{f_t^+ - f(\mathbf{x}), 0\}, \quad (4)$$

where f_t^+ denotes the best current objective value. The sample point that generates f_t^+ is denoted as \mathbf{x}_t^+ . The EI acquisition function is defined as the expectation of (4) conditioned on t samples, with the expression:

$$EI_t(\mathbf{x}) = (f_t^+ - \mu_t(\mathbf{x}))\Phi(z_t(\mathbf{x})) + \sigma_t(\mathbf{x})\phi(z_t(\mathbf{x})), \quad (5)$$

where $z_t(\mathbf{x}) = \frac{f_t^+ - \mu_t(\mathbf{x})}{\sigma_t(\mathbf{x})}$. The functions ϕ and Φ are the PDF and CDF of the standard normal distribution, respectively. For ease of reference, we refer to $f_t^+ - \mu_t(\mathbf{x})$ and $\sigma_t(\mathbf{x})$ as the exploitation and exploration part of $EI_t(\mathbf{x})$, respectively (see also Appendix A for more discussions). A commonly used function in the analysis of EI is the function $\tau : \mathbb{R} \rightarrow \mathbb{R}$, defined as

$$\tau(z) = z\Phi(z) + \phi(z). \quad (6)$$

Thus, the τ form of EI can be written as $EI_t(\mathbf{x}) = \sigma_t(\mathbf{x})\tau(z_t(\mathbf{x}))$. The next sample is chosen by maximizing the acquisition function over C , *i.e.*,

$$\mathbf{x}_t = \operatorname{argmax}_{\mathbf{x} \in C} EI_{t-1}(\mathbf{x}), \quad (7)$$

breaking ties arbitrarily [11]. The practical EGO algorithm is given in Algorithm 1.

Algorithm 1 Practical EGO

- 1: Choose $k(\cdot, \cdot)$ and T_0 initial samples $\mathbf{x}_i, i = 0, \dots, T_0$. Observe f_i . Train the initial GP.
 - 2: **for** $t = T_0 + 1, T_0 + 2, \dots$ **do**
 - 3: Choose \mathbf{x}_t using (7).
 - 4: Observe $f(\mathbf{x}_t)$.
 - 5: Update the surrogate model using $\mathbf{x}_{1:t}$ and $\mathbf{f}_{1:t}$.
 - 6: **if** Evaluation budget is exhausted **then**
 - 7: Exit
 - 8: **end if**
 - 9: **end for**
-

2.3 Additional Background

Denote the optimal function value as $f(\mathbf{x}^*)$, where \mathbf{x}^* is a global minimum on C , *i.e.*, $\mathbf{x}^* \in \underset{\mathbf{x} \in C}{\operatorname{argmin}} f(\mathbf{x})$.

The instantaneous regret r_t is defined as

$$r_t = f(\mathbf{x}_t) - f(\mathbf{x}^*) \geq 0. \quad (8)$$

The cumulative regret R_T after T samples is defined as

$$R_T = \sum_{t=1}^T r_t = \sum_{t=1}^T [f(\mathbf{x}_t) - f(\mathbf{x}^*)]. \quad (9)$$

In order to derive the cumulative regret upper bound, we use the well-established maximum information gain results [9, 41]. Information gain measures the informativeness of a set of sample points in C about f . The maximum information gain γ_t is defined in Definition A.3 in Appendix A. It is often used to bound the summation of posterior standard deviation $\sigma_{t-1}(\mathbf{x}_t)$ and is dependent on the choice of the kernel [41]. We note that the upper bound on the sum of $\sigma_{t-1}(\mathbf{x}_t)$ is dependent on both γ_t and ϵ . Moreover, the bound on γ_t itself is also dependent on ϵ , the kernel, C , and d . The latest bounds on γ_t in literature for common kernels such as the SE kernel and Matérn kernel can be found in [20, 46] and Lemma A.5.

3 Regret Bound

In this section, we present our regret bounds of practical EGO. We start with preliminary results required for the analysis in Section 3.1. Then, the new instantaneous regret bound is given in Section 3.2. Finally, the cumulative regret bound is established in Section 3.3.

3.1 Assumptions and Preliminary Results

Throughout this paper, we consider the frequentist setting. That is, f lies in the RKHS of $k(\cdot, \cdot)$, a com-

mon assumption in literature [41], whose definition is in Section A in the appendix. The formal assumption is given below.

Assumption 3.1. The function f lies in the RKHS, denoted as $\mathcal{H}_k(C)$, associated with the bounded kernel $k(\mathbf{x}, \mathbf{x}')$ with the norm $\|\cdot\|_{H_k}$. The kernel satisfies $k(\mathbf{x}, \mathbf{x}') \leq 1, \forall \mathbf{x}, \mathbf{x}' \in C$, and $k(\mathbf{x}, \mathbf{x}) = 1$. The RKHS norms of the kernels are bounded above by constant $B > 0$, *i.e.*, $\|f\|_{H_k} \leq B$. The set C is compact.

To help analyze r_t , we present Lemmas B.1 to B.6 on the properties of GP and EI. We briefly summarize some of them here, and leave the theory statements and proofs in Appendix B. The monotonicity of function τ (6) and its derivative are given in Lemma B.1 [23]. Lemma B.2 states the relationship between $\Phi(z)$ and $\tau(z)$ when $z < 0$. In Lemma B.3, we establish simple but useful bounds of for $\frac{EI_{t-1}(\mathbf{x})}{\sigma_{t-1}(\mathbf{x})}$. Since $EI_{t-1}(\mathbf{x}) = \sigma_{t-1}(\mathbf{x})\tau(z_{t-1}(\mathbf{x}))$, the above three lemmas can be used to bound $EI_{t-1}(\mathbf{x})$. In Lemma B.4, $EI_{t-1}(\mathbf{x})$ is shown to be monotonically increasing with respect to both its exploitation $f_{t-1}^+ - \mu_{t-1}(\mathbf{x})$ and exploration $\sigma_{t-1}(\mathbf{x})$. Lemma B.2, B.3 and B.4 are used to quantify the exploration and exploitation trade-off properties in Section 3.2.

A lower bound on $f_{t-1}^+ - \mu_{t-1}(\mathbf{x}_t)$ when $EI_{t-1}(\mathbf{x})$ is bounded below is given in Lemma B.5 [32]. The global lower bound for $\sigma_{t-1}(\mathbf{x})$ with nugget is given in Lemma B.6. These two lemmas are used to establish the lower bound for $EI_{t-1}(\mathbf{x}_t)$ and subsequently a lower bound for $f_{t-1}^+ - \mu_{t-1}(\mathbf{x}_t)$, which appears in an intermediate upper bound for r_t .

Next, we establish the bound on $|I_{t-1}(\mathbf{x}) - EI_{t-1}(\mathbf{x})|$, an important step leading to the bound on r_t . Under the noise-free frequentist setting, the upper bound on $|f(\mathbf{x}) - \mu_{t-1}(\mathbf{x})|$ has been established in literature (see *e.g.*, [41]). We note that while practical EGO uses ϵ in its posterior calculations, the confidence interval of $|f(\mathbf{x}) - \mu_{t-1}(\mathbf{x})| \leq B\sigma_{t-1}(\mathbf{x})$ continue to hold [9]. The effect of ϵ on the upper bound is reflected in the increased $\sigma_{t-1}(\mathbf{x})$. Specifically, $|f(\mathbf{x}) - \mu_{t-1}(\mathbf{x})| \leq B\sigma_{t-1}(\mathbf{x})$ holds at given $\mathbf{x} \in C$ and $t \in \mathbb{N}$, as stated in Lemma B.7. Then, using this bound, we can establish the bounds on $I_{t-1}(\mathbf{x})$ and $EI_{t-1}(\mathbf{x})$ in Lemma B.9 through Lemma B.8.

3.2 Instantaneous Regret Bound

In this section, we derive the instantaneous regret upper bounds of r_t in terms of the posterior standard deviations $\sigma_{t-1}(\mathbf{x}_t)$ and additional exploitation terms, where the former's sum can be bounded with maximum information gain γ_t .

Lemma 3.2. *The practical EGO generates the instantaneous regret bound*

$$r_t \leq c_{B1} \max\{f_{t-1}^+ - f(\mathbf{x}_t), 0\} + (c_{B\epsilon}(\epsilon, t) + B + c_B(B + \phi(0)))\sigma_{t-1}(\mathbf{x}_t), \quad (10)$$

where $c_{B\epsilon}(\epsilon, t) = \log^{1/2}\left(\frac{t+\epsilon}{2\pi\epsilon\tau^2(-B)}\right)$, $c_B = \frac{\tau(B)}{\tau(-B)}$ and $c_{B1} = \max\left\{\frac{\tau(B)}{\tau(-B)} - 1, 0\right\}$.

Proof Sketch for Lemma 3.2. We consider two different cases: $f_{t-1}^+ - f(\mathbf{x}_t) \leq 0$ and $f_{t-1}^+ - f(\mathbf{x}_t) > 0$. For the first case, where $f_{t-1}^+ - f(\mathbf{x}_t) \leq 0$, we use the bound on $|f(\mathbf{x}) - \mu_{t-1}(\mathbf{x})|$ (Lemma B.7) and Lemma B.9 to obtain an upper bound of r_t : $\mu_{t-1}(\mathbf{x}_t) - f_{t-1}^+ + c_B EI_{t-1}(\mathbf{x}_t) + B\sigma_{t-1}(\mathbf{x}_t)$, where $c_B = \frac{\tau(B)}{\tau(-B)}$. To derive an upper bound for $\mu_{t-1}(\mathbf{x}_t) - f_{t-1}^+$, we establish a positive lower bound $\mathcal{O}\left(\frac{1}{\sqrt{t}}\right)$ of $EI_{t-1}(\mathbf{x}_t)$ at $\forall t \in \mathbb{N}$. We consider $EI_{t-1}(\mathbf{x}^*)$ and show that $EI_{t-1}(\mathbf{x}^*) \geq \sigma_{t-1}(\mathbf{x}^*)\tau(-B)$ using the global lower bound on $\sigma_{t-1}(\mathbf{x})$ mentioned in Section 3.1 (Lemma B.6). Then, the upper bound for $\mu_{t-1}(\mathbf{x}_t) - f_{t-1}^+$ can be derived by the properties of EI (Lemma B.5). The upper bound on r_t becomes $(c_{B\epsilon}(\epsilon, t) + B + c_B(\phi(0) + B))\sigma_{t-1}(\mathbf{x}_t)$, where $c_{B\epsilon}(\epsilon, t) = \log^{1/2}\left(\frac{t+\epsilon}{2\pi\tau^2(-B)\epsilon}\right)$.

For the second case where $f_{t-1}^+ - f(\mathbf{x}_t) \geq 0$, from Lemma B.9, we have the upper bound for r_t : $f(\mathbf{x}_t) - f_{t-1}^+ + c_B EI_{t-1}(\mathbf{x}_t)$. We can further bound $EI_{t-1}(\mathbf{x}_t)$ via the bounds on $|f(\mathbf{x}) - \mu_{t-1}(\mathbf{x})|$ (Lemma B.7) and the properties of EI (Lemma B.3). Thus, the upper bound for r_t becomes $(c_B - 1)(f_{t-1}^+ - f(\mathbf{x}_t)) + c_B(B + \phi(0))\sigma_{t-1}(\mathbf{x}_t)$. Combining the bounds in both cases leads to (10) in Lemma 3.2.

Remark 3.3 (Use of ϵ in Lemma 3.2). In addition to improved numerical stability and statistical properties mentioned in Section 1, ϵ plays an important role in the analysis of r_t . Specifically, the upper bound on $\mu_{t-1}(\mathbf{x}_t) - f_{t-1}^+$ requires a positive lower bound on $EI_{t-1}(\mathbf{x}_t)$. The use of ϵ provides a positive global lower bound for the posterior standard deviation $\sigma_{t-1}(\mathbf{x})$, which leads to the positive lower bound on $EI_{t-1}(\mathbf{x}_t)$. Without ϵ , at previous sample points $\mathbf{x}_i, i = 1, \dots, t-1$, we have $\sigma_{t-1}(\mathbf{x}_i) = 0$ and $EI_{t-1}(\mathbf{x}_i) = 0$. Since it is possible that $\mathbf{x}_i = \mathbf{x}^*$ for some i , we can no longer guarantee a positive lower bound for $EI_{t-1}(\mathbf{x}^*)$, a critical step towards the lower bound on $EI_{t-1}(\mathbf{x}_t)$. Thus, we can no longer obtain a desirable upper bound for $\mu_{t-1}(\mathbf{x}_t) - f_{t-1}^+$. Intuitively, $\epsilon > 0$ means that there is still uncertainty recognized by the GP model, albeit decreasing, at previous sample points, making it more likely that the next sample is chosen close to existing samples, when some of them are already close to \mathbf{x}^* .

Remark 3.4 (Exploitation term in instantaneous regret bound). The instantaneous regret upper bound in Lemma 3.2 contains the exploitation term $\max\{f_{t-1}^+ - f(\mathbf{x}_t), 0\}$, which is a novelty for instantaneous regret bound, as far as we know. For instance, the instantaneous regret bound for UCB only has the exploration terms involving $\sigma_{t-1}(\mathbf{x}_t)$. We elaborate our techniques to bound the sum of $\max\{f_{t-1}^+ - f(\mathbf{x}_t), 0\}$ in Section 3.3.

3.3 Cumulative Regret Bound

In this section, we present the cumulative regret bound of practical EGO. The following lemma establishes the bound based on Lemma 3.2.

Lemma 3.5. *The cumulative regret bound of practical EGO satisfies*

$$R_T \leq 2c_{B1}B + (c_{B\epsilon}(\epsilon, T) + B + c_B(B + \phi(0)))\sqrt{C_\gamma(\epsilon)T\gamma_T}, \quad (11)$$

where $c_{B\epsilon}(\epsilon, t) = \log^{\frac{1}{2}}\left(\frac{t+\epsilon}{2\pi\epsilon\tau^2(-B)}\right)$, $C_\gamma(\epsilon) = \frac{2}{\log(1+1/\epsilon)}$, $c_B = \frac{\tau(B)}{\tau(-B)}$, and $c_{B1} = \max\left\{\frac{\tau(B)}{\tau(-B)} - 1, 0\right\}$.

Proof Sketch for Lemma 3.5. From Lemma 3.2 and the definition of R_T , we need to bound the sum of the exploitation term $\sum_{t=1}^T \max\{f_{t-1}^+ - f(\mathbf{x}_t), 0\}$ and $\sum_{t=1}^T c_{B\epsilon}(\epsilon, t)\sigma_{t-1}(\mathbf{x}_t)$, given that the sum of the remaining terms are obvious. To bound the first sum, we construct the subsequence $\{\mathbf{x}_{t_i}\}$ of $\{\mathbf{x}_t\}$ for all \mathbf{x}_t that satisfies $f_{t-1}^+ - f(\mathbf{x}_t) > 0$. Using $f_{t_i}^+ \leq f(\mathbf{x}_{t_i})$ and the fact that $t_{i-1} \leq t_i - 1$, we can write $f_{t_{i-1}}^+ - f(\mathbf{x}_{t_i}) + f_{t_{i+1}-1}^+ - f(\mathbf{x}_{t_{i+1}}) \leq f(\mathbf{x}_{t_{i-1}}) - f(\mathbf{x}_{t_{i+1}}) \leq 2B$. Using this technique and summing up all t_i lead to the bound on $\sum_{t=1}^T \max\{f_{t-1}^+ - f(\mathbf{x}_t), 0\}$.

For the latter term, using the maximum information gain γ_t from Lemma A.4 suffices as $\sum_{t=1}^T c_{B\epsilon}(\epsilon, t)\sigma_{t-1}(\mathbf{x}_t) \leq c_{B\epsilon}(\epsilon, T)\sum_{t=1}^T \sigma_{t-1}(\mathbf{x}_t)$.

The rate of the cumulative regret upper bound of practical EGO is stated in the following theorem.

Theorem 3.6. *The practical EGO algorithm leads to the cumulative regret upper bound*

$$R_T = \mathcal{O}(\log^{1/2}(T)T^{1/2}\sqrt{\gamma_T}).$$

For SE kernel, $R_T = \mathcal{O}(T^{1/2}\log^{(d+2)/2}(T))$. For Matérn kernels ($\nu > \frac{1}{2}$), $R_T = \mathcal{O}(T^{\frac{\nu+d}{2\nu+d}}\log^{\frac{2\nu+0.5d}{2\nu+d}}(T))$.

From Theorem 3.6, if γ_T of the chosen kernel is sublinear, practical EGO is no-regret.

Remark 3.7. Our analysis framework does not directly apply to the cumulative regret of EGO (without ϵ). As mentioned in Remark 3.3, EGO has $\sigma_{t-1}(\mathbf{x}_i) = 0, i = 1, \dots, t-1$, and thus $EI_{t-1}(\mathbf{x}_i) = 0$ at previous sample points. Therefore, we cannot obtain a lower bound of $EI_{t-1}(\mathbf{x}_t)$ via $EI_{t-1}(\mathbf{x}^*)$. Consequently, the current upper bound on $\mu_{t-1}(\mathbf{x}_t) - f_{t-1}^+$ cannot be obtained for EGO. Determining whether EGO is a no-regret algorithm is a topic for future research and can be considered a limitation of this paper.

4 Effect of the Nugget

In this section, we discuss the impact of the nugget ϵ on practical EGO. The effect of ϵ on the properties of GP such as the likelihood have been studied previously [2]. Our focus is thus on how ϵ can change EI and the cumulative regret bounds of practical EGO.

First, we briefly demonstrate the effect ϵ can have on the maximum of the EI function, *i.e.*, $EI_{t-1}(\mathbf{x}_t)$, via a 2-dimensional example. We use the Branin function (see example 4 in Section 5) and the GP model from scikit-learn [33]. We train the GP with $\epsilon = 10^{-2}$, $\epsilon = 10^{-6}$, $\epsilon = 10^{-10}$, and without nuggets using the same 50 samples (25 initial samples and 25 iterations of practical EGO where we set $\epsilon = 10^{-6}$), and plot the contours of EI in Figure 1. We note that the maximum level of the EI value colorbar corresponds to the maximum of EI_{50} in each contour plot.

Remark 4.1. We remark that while given 50 samples, GP with no nugget does not have numerical issues, we encounter Cholesky decomposition failure when inverting the covariance matrix using 25 random initial samples and around 75 samples generated from practical EGO runs.

It is clear from Figure 1 that ϵ impacts $EI_{t-1}(\mathbf{x}_t)$, of which a positive lower bound is needed for the bound on r_t (see proof of Lemma 3.2). In this example, the impact is relatively small when ϵ is small, *e.g.*, 10^{-10} . Consistent with our analysis in Section 3, ϵ ensures a lower bound on $\sigma_{t-1}(\mathbf{x})$ and thus a lower bound of $EI_{t-1}(\mathbf{x}_t)$. This is reflected in the increased value of $EI_{t-1}(\mathbf{x}_t)$ as ϵ increases. We emphasize that the effect of ϵ is dependent on multiple factors such as the sample set, the function, the kernel, etc, and therefore, Figure 1 is one illustrative example. For instance, if one uses all 50 samples generated by random sampling in the example above, the effect of ϵ would be much less prominent since the samples are more evenly spaced out, as shown in Figure 5 in appendix.

Next, we discuss the effect of the nugget on the regret bound from the theoretical perspective. From Lemma 11, ϵ appears in the cumulative regret upper

bound

$$2c_{B1}B + (c_{B\epsilon}(\epsilon, T) + B + c_B(B + \phi(0)))\sqrt{C_\gamma(\epsilon)T\gamma_T(\epsilon)} \quad (12)$$

through $c_{B\epsilon}(\epsilon, T)$, $C_\gamma(\epsilon)$, as well as $\gamma_T(\epsilon)$.

To make matters complicated, $c_{B\epsilon}(\epsilon, T)$ decreases, while $C_\gamma(\epsilon)$ increases, as ϵ increases. Further, the dependence of γ_T on ϵ is kernel specific. Thus, the impact of ϵ on (12) is complex and dependent on the kernel. Here, we provide an answer to this challenging question for SE and Matérn kernels via the bounds on γ_T in [20], as stated in Lemma E.1. From Lemma E.1 for SE and Matérn kernels, the upper bound on $\gamma_T(\epsilon)$ decreases as ϵ increases.

For simplicity, we consider constant length scale l in both kernels. Further, since the nugget is often small in nature, we focus on the case where T/ϵ is large. The effect of the nugget ϵ on (12) for SE kernel is presented next.

Theorem 4.2. *Under the conditions of Lemma E.2 and $T/\epsilon \gg 1$, for SE kernel at given T ,*

(1) if

$$(d+1)\log(1+1/\epsilon) > \log(1+T/\epsilon), \quad (13)$$

and $\log(1+T/\epsilon) \gg \max\{C_{dl}^2, C_{dl}^3, C_R^2, C_R^3, C_R^3, d\}$, then (12) decreases as ϵ increases. The constants are defined in Lemma E.1 and Lemma E.2.

(2) if

$$(d+2)\log(1+1/\epsilon) < (1+\epsilon/T)/(1+\epsilon)\log(1+T/\epsilon), \quad (14)$$

then (12) increases as ϵ increases.

Next, we consider the Matérn kernels ($\nu > \frac{1}{2}$).

Theorem 4.3. *Under the conditions of Lemma E.3 where $T/\epsilon \gg 1$, for Matérn kernel ($\nu > \frac{1}{2}$),*

(1) if

$$\log(1+1/\epsilon)d/(2\nu+d) > (1+1/C_{d\nu}^2), \text{ and } C_\nu^1 C_{d\nu}^1 C_\nu^3 \log(1+1/\epsilon) \log(1+2T/\epsilon) > C, \quad (15)$$

then (12) decreases with increasing ϵ . The constants are defined in Lemma E.1 and Lemma E.3.

(2) if

$$\log(1+1/\epsilon) \left[\frac{d}{2\nu+d} + C_\nu^1 C_\nu^3 + \left(\frac{4\nu+d}{2\nu+d} + C_\nu^1 \right) \frac{1}{\log(T/\epsilon)} \right] < 1/(1+\epsilon), \quad (16)$$

then (12) increases with increasing ϵ .

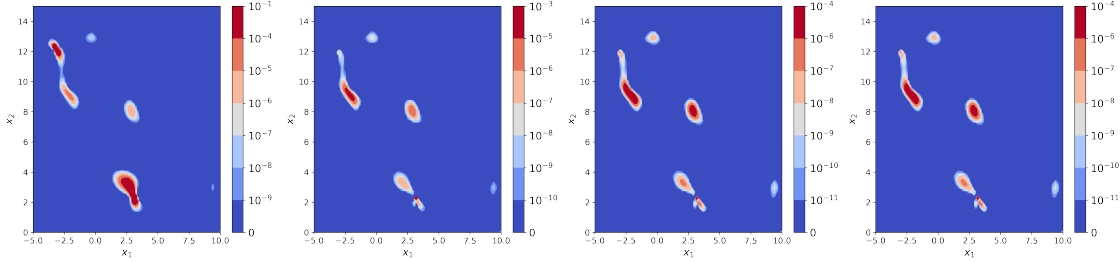


Figure 1: Illustrative example of EI contour of the Branin function with 50 samples. From left to right: contour plots for $\epsilon = 10^{-2}$, $\epsilon = 10^{-6}$, $\epsilon = 10^{-10}$, and no nugget. The maximum EI_{50} value from left to right: 2.53×10^{-2} , 1.90×10^{-4} , 4.72×10^{-5} , and 4.72×10^{-5} .

Remark 4.4. The constants in Theorem 4.2 and 4.3 are dependent on d , C , and the fixed hyper-parameter l . Readers are referred to Lemma E.1, E.2, and E.3 for their definitions. When T/ϵ is sufficiently large, the conditions involving the constants are satisfied.

Remark 4.5. We note that case 2 in both theorems might not be satisfied when T is small (ϵ also small to maintain a large T/ϵ), as well as when d is large. Further, for any given T , for SE kernel, it is possible that neither (13) nor (14) is satisfied. In such cases, the constants play an important role in how ϵ affect (12). Similar conclusions can be drawn for Matérn kernels.

Theorem 4.2 and 4.3 show that to obtain a tighter cumulative regret bound, ϵ should stay within a reasonable range. When ϵ is small, conditions (1) for both kernels are more likely to be satisfied and (12) increases as ϵ decreases. When ϵ is large, conditions (2) are more likely to be satisfied and (12) increases as ϵ increases.

Intuitively, if ϵ is too large, the posterior variance is inflated too much and EI could emphasize too much on exploration. On the other hand, if ϵ is too small, practical EGO behaves closer to EGO, which might not be no-regret. In addition, an ϵ too small risks not resolving numerical stability issues. We emphasize that our analysis is based on state-of-the-art cumulative regret bound (12), and not the cumulative regret itself.

To better illustrate our results, we choose an example set of constants and plot the cumulative regret bound with ϵ . Let $C_{dt}^1 = C_{dt}^2 = C_{dt}^3 = 1$, $d = 2$, $B = 1$ for the SE kernel. For the Matérn kernel, let $\nu = 2.5$, $d = 3$, $C_\nu = 1$, $C_{d\nu l1} = 1$, $C_{d\nu l2} = 1$, and $C = 1$. The rest of the constants can be deduced from these chosen ones. We plot (12) with ϵ for SE kernel in Figure 2 and the one for Matérn kernel in Figure 4 in the appendix. We mark when the conditions for the two cases are met in Theorem 4.2 and 4.3.

The plots clearly demonstrate our theoretical conclusions on the effect of ϵ . We note that the inequali-

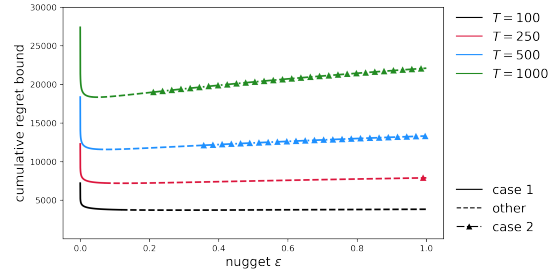


Figure 2: Cumulative regret upper bound with nugget ϵ at different T and selected constants for SE kernel. The case “other” means neither the conditions for case 1 nor those for case 2 are satisfied.

ties (13), (14), (15), and (16) are much relaxed to allow for simpler forms. It is clear that when T is small, the second case conditions for both kernels might not be satisfied. This does not mean that the cumulative regret bound is not increasing with ϵ . However, when T is small the effect of ϵ becomes more complicated to summarize and highly dependent on constants.

5 Numerical Experiments

In this section, we perform numerical experiments of practical EGO with varying nugget values on widely used test problems to demonstrate the empirical validity of our theories. We consider two groups of functions. First, we test functions sampled from GPs with known SE and Matérn kernels ($\nu = 2.5$) using fixed hyperparameters. These problems are designed to minimize the effect of misspecification of kernels or hyperparameter optimization of GP. Second, we consider commonly used synthetic functions.

For the first group of functions, we use 20 and 40 initial design points for 2D and 4D problems, respectively, followed by 200 additional observations acquired iteratively via practical EGO. We use three ϵ

Table 1: The average accumulative regret for different iteration over 20 macro-replications.

D	KERNEL	ϵ	T=1	T=50	T=100	T=200
2	SE	10^{-10}	0.596	0.091	0.058	0.040
2	SE	10^{-6}	0.596	0.141	0.101	0.076
2	SE	10^{-4}	0.596	0.153	0.120	0.097
2	MATÉRN	10^{-10}	0.393	0.061	0.031	0.016
2	MATÉRN	10^{-6}	0.393	0.055	0.028	0.015
2	MATÉRN	10^{-4}	0.393	0.054	0.028	0.016
4	SE	10^{-10}	1.422	0.775	0.626	0.440
4	SE	10^{-6}	1.422	0.788	0.640	0.440
4	SE	10^{-4}	1.422	0.799	0.693	0.528
4	MATÉRN	10^{-10}	0.857	0.458	0.296	0.183
4	MATÉRN	10^{-6}	0.857	0.493	0.291	0.184
4	MATÉRN	10^{-4}	0.857	0.474	0.292	0.184

values for each problem, 10^{-10} , 10^{-6} , and 10^{-4} . The GP hyperparameters were kept fixed to the original values used for sampling. The results are shown in Table 1.

For each problem, the average cumulative regret, *i.e.*, R_T/T , declines as optimization progresses. For Matérn kernels and SE kernel in 4D, the observed regret behavior with respect to ϵ align well with our theoretical regret bound predictions, namely that regret bounds do not change monotonically with ϵ and there might exist a range where ϵ should be chosen. The SE kernels in 2D however, show a smaller regret for smaller ϵ . We note that this is not contradictory to our conclusion, as it is based on the upper bound of the regret.

For synthetic problems, we choose five examples and three nugget values $\epsilon = 10^{-2}$, $\epsilon = 10^{-4}$, and $\epsilon = 10^{-6}$ for each problem. From example 1 to 5, the objective functions are the Rosenbrock function, the six-hump camel function, the Hartmann6 function, the Branin function, and the Michalewicz function [31, 35]. The mathematical expressions of our test problems are given in Section F in the appendix. The results for the five examples are plotted in Figure 3.

The synthetic examples are implemented using GP models in scikit-learn. Each example is run 100 times to account for stochasticity. For the two-dimensional examples 1, 2, 4, 5, five initial Latin hypercube samples are used. For the six-dimensional problem, example 3, we choose 50 initial Latin hypercube samples due to the increase in dimension. For example 1, 2, 3, SE kernel is used, while Matérn kernel with $\nu = 2.5$ is used for example 4 and 5, for a demonstration of both kernels mentioned in our theories. The median of the average cumulative regret among the 100 runs is reported against the number of iterations. The 25th and 75th percentile results are shown in Section F in

the appendix. The computational budget is 200 optimization iterations for examples 1,2, and 4 and 100 for examples 3, due to the increased dimension and computational cost. For example 5, we also terminate at 100 optimization iterations as R_T/T is sufficiently small.

For all of our examples, practical EGO displays no-regret convergence behavior and is capable of finding the optimal solution rather efficiently, supporting our theoretical results. The different values of ϵ again align well with the regret bound theory, with $\epsilon = 10^{-4}$ appearing to generate lowest regret in 3 out of the 5 examples.

6 Conclusions

In this paper, we establish the novel instantaneous regret bound and the first cumulative regret upper bound for practical EGO, which is the default implementation of EGO in many available software packages. We show that it is a no-regret algorithm for kernels including SE and Matérn kernels. Our analysis thus provides cumulative regret theories on one of the most widely used BO algorithms. Further, we provide theoretical guidelines on the choice of the nugget in that ϵ too large can lead to a worse cumulative regret upper bound. In practice, we anticipate the choice of ϵ to be influenced by other factors beyond our theoretical results such as the computational budget and the kernel.

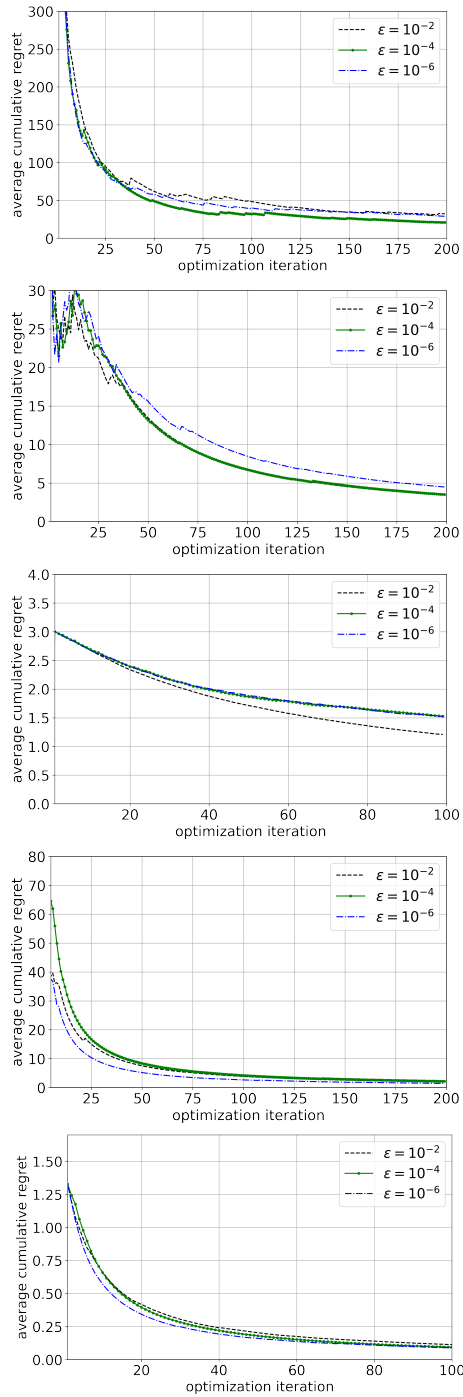


Figure 3: Median average cumulative regret bound for practical EGO with ϵ values 10^{-2} , 10^{-4} , and 10^{-6} for five examples. From top to bottom: Rosenbrock, Six-hump camel, Hartmann6, Branin, Michalewicz functions.

A Background

We first define an equivalent form of EI (5). We distinguish between its exploration and exploitation parts and define the *trade-off* form $EI(a, b) : \mathbb{R} \times \mathbb{R} \rightarrow \mathbb{R}$ as

$$EI(a, b) = a\Phi\left(\frac{a}{b}\right) + b\phi\left(\frac{a}{b}\right), \quad (17)$$

where $b \in (0, 1]$. One can view a and b as two independent variables. For a given \mathbf{x} , if $a_t = f_t^+ - \mu_t(\mathbf{x})$ and $b_t = \sigma_t(\mathbf{x}) \in [0, 1]$, then $EI(a_t, b_t) = EI_t(\mathbf{x})$. Hence, we refer to $f_t^+ - \mu_t(\mathbf{x})$ and $\sigma_t(\mathbf{x})$ the exploitation and exploration parts of EI_t , respectively.

The definition of RKHS is given below.

Definition A.1. Consider a positive definite kernel $k : \mathcal{X} \times \mathcal{X} \rightarrow \mathbb{R}$ with respect to a finite Borel measure supported on \mathcal{X} . A Hilbert space H_k of functions on \mathcal{X} with an inner product $\langle \cdot, \cdot \rangle_{H_k}$ is called a RKHS with kernel k if $k(\cdot, \mathbf{x}) \in H_k$ for all $\mathbf{x} \in \mathcal{X}$, and $\langle f, k(\cdot, \mathbf{x}) \rangle_{H_k} = f(\mathbf{x})$ for all $\mathbf{x} \in \mathcal{X}, f \in H_k$. The induced RKHS norm $\|f\|_{H_k} = \sqrt{\langle f, f \rangle_{H_k}}$ measures the smoothness of f with respect to k .

Union bound is given in the next lemma.

Lemma A.2. For a countable set of events A_1, A_2, \dots , we have

$$\mathbb{P}\left(\bigcup_{i=1}^{\infty} A_i\right) \leq \sum_{i=1}^{\infty} \mathbb{P}(A_i).$$

To use the maximum information gain, we consider a Gaussian observation noise $\eta \sim \mathcal{N}(0, \epsilon)$. If such an i.i.d. noise exists, at sample point \mathbf{x}_t , we have the observation $y_t = f(\mathbf{x}_t) + \eta_t$. The maximum information gain can now be defined below.

Definition A.3. Consider a set of sample points $A \subset C$. Given \mathbf{x}_A and its function values $\mathbf{f}_A = [f(\mathbf{x})]_{\mathbf{x} \in A}$, the mutual information between \mathbf{f}_A and the observation \mathbf{y}_A is $I(\mathbf{y}_A; \mathbf{f}_A) = H(\mathbf{y}_A) - H(\mathbf{y}_A | \mathbf{f}_A)$, where H is the entropy. The maximum information gain γ_T after T samples is $\gamma_T = \max_{A \subset C, |A|=T} I(\mathbf{y}_A; \mathbf{f}_A)$.

Readers are referred to [10, 41] for a detailed discussion of the maximum information gain. Here, we emphasize that practical EGO assumes no observation noise. However, we can continue to use maximum information gain as an analytic tool to bound $\sum_{t=1}^T \sigma_{t-1}(\mathbf{x}_t)$. Indeed, $\sigma_{t-1}(\mathbf{x})$ of practical EGO is the same as that of GP with Gaussian noise $\mathcal{N}(0, \epsilon)$.

The following lemmas are well-established results from [41] on the information gain and variances.

Lemma A.4. The sum of posterior standard deviation at sample points $\sigma_{t-1}(\mathbf{x})$ satisfies

$$\sum_{t=1}^T \sigma_{t-1}(\mathbf{x}_t) \leq \sqrt{C_\gamma(\epsilon) T \gamma_T(\epsilon)}, \quad (18)$$

where $C_\gamma(\epsilon) = 2/\log(1 + \epsilon^{-1})$.

Here, we emphasize that the maximum information gain is dependent on the nugget ϵ . The state-of-the-art rates of γ_t for two commonly used kernels are given below.

Lemma A.5 ([20, 46]). For a GP with t samples, the SE kernel has $\gamma_t = \mathcal{O}(\log^{d+1}(t))$, and the Matérn kernel with smoothness parameter $\nu > 0$ has $\gamma_t = \mathcal{O}(t^{\frac{d}{2\nu+d}} \log^{\frac{2\nu}{2\nu+d}}(t))$.

Before concluding the section, we state the straightforward bound of f on C as a lemma for easy reference.

Lemma A.6. The function f is bounded by B , i.e., $|f(\mathbf{x})| \leq B$ for all $\mathbf{x} \in C$.

Proof. From our assumption on the kernel $k(\mathbf{x}, \mathbf{x}) = 1$, we can write

$$|f(\mathbf{x})| \leq \|f\|_{H_k} k(\mathbf{x}, \mathbf{x}) \leq B. \quad (19)$$

□

B Preliminary Results

First, we state a property of $\tau(\cdot)$ in (6) below.

Lemma B.1. *The function $\tau(z)$ is monotonically increasing in z and $\tau(z) > 0$ for $\forall z \in \mathbb{R}$. The derivative of $\tau(z)$ is $\Phi(z)$.*

Proof. From the definition of $\tau(z)$, we can write

$$\tau(z) = z\Phi(z) + \phi(z) > \int_{-\infty}^z u\phi(u)du + \phi(z) = -\phi(u)|_{-\infty}^z + \phi(z) = 0. \quad (20)$$

Given the definition of $\phi(u)$,

$$\frac{d\phi(u)}{du} = \frac{1}{\sqrt{2\pi}}e^{-\frac{u^2}{2}}(-u) = -\phi(u)u. \quad (21)$$

Thus, the derivative of τ is

$$\frac{d\tau(z)}{dz} = \Phi(z) + z\phi(z) - \phi(z)z = \Phi(z) > 0. \quad (22)$$

□

Another lemma on τ and Φ is given below.

Lemma B.2. *Given $z > 0$, $\Phi(-z) > \tau(-z)$.*

Proof. Define $q(z) = \Phi(-z) - \tau(-z)$. Using integration by parts, we have

$$\Phi(z) = \int_{-\infty}^z \phi(u)du > \int_{-\infty}^z \phi(u) \left(1 - \frac{3}{u^4}\right) du = -\frac{\phi(z)}{z} + \frac{\phi(z)}{z^3}. \quad (23)$$

Replacing z with $-z$ in (23),

$$\phi(-z) \left(\frac{1}{z} - \frac{1}{z^3}\right) < \Phi(-z). \quad (24)$$

Multiplying both sides in (24) by $1 + z$,

$$(1 + z)\Phi(-z) > \phi(-z) \frac{z^2 - 1}{z^3} (1 + z) = \phi(-z) \left(1 + \frac{z^2 - z - 1}{z^3}\right). \quad (25)$$

Thus, if $z > \frac{1+\sqrt{5}}{2}$, then the right-hand-side of (25) $> \phi(-z)$ and

$$q(z) := \Phi(-z) - \tau(-z) = (1 + z)\Phi(-z) - \phi(-z) > 0. \quad (26)$$

Therefore, in the following, we focus on $z \in (0, \frac{1+\sqrt{5}}{2}]$. We analyze $q(z)$ using its derivatives. Taking the derivative of q , by Lemma B.1,

$$\frac{dq(z)}{dz} = -\phi(-z) + \Phi(-z) := q'(z). \quad (27)$$

Further, the derivative of $q'(z)$ is

$$\frac{d^2q(z)}{dz^2} = \frac{dq'(z)}{dz} = -\phi(-z) + \phi(-z)z = \phi(z)(z - 1). \quad (28)$$

For $z > 1$, $\frac{d^2q(z)}{dz^2} > 0$. For $0 < z < 1$, $\frac{d^2q(z)}{dz^2} < 0$. Thus, $q'(z)$ is monotonically decreasing for $0 < z < 1$ and then monotonically increasing for $z > 1$. We first consider $q'(z)$ for $0 < z < 1$. We know that by simple algebra, $q'(0) = \Phi(0) - \phi(0) > 0$ and $q'(1) = \Phi(-1) - \phi(-1) < 0$. Thus, there exists a $0 < \bar{z} < 1$ so that $q'(\bar{z}) = 0$. Next, for $z > 1$, from Lemma B.1, we can write

$$q'(z) = \Phi(-z) - \phi(-z) < z\Phi(-z) - \phi(-z) = -\tau(-z) < 0. \quad (29)$$

Therefore, $0 < \bar{z} < 1 < \frac{1+\sqrt{5}}{2}$ is a unique stationary point such that $q'(\bar{z}) = 0$. Thus, $q'(z) > 0$ for $0 < z < \bar{z} < \frac{1+\sqrt{5}}{2}$ and $q'(z) < 0$ for $z > \bar{z}$. This means that for $0 < z < \bar{z}$, $q(z)$ is monotonically increasing. For $\bar{z} < z < \frac{1+\sqrt{5}}{2}$, $q(z)$ is monotonically decreasing. Therefore, $q(z) > \min\{q(0), q(\frac{1+\sqrt{5}}{2})\}$ for $z \in (0, \frac{1+\sqrt{5}}{2})$. Since $q(0) > 0$ and $q(\frac{1+\sqrt{5}}{2}) > 0$, $q(z) > 0$ for $z \in (0, \frac{1+\sqrt{5}}{2})$. Combined with (26), the proof is complete. □

The next lemma contains basic inequalities for EI_t .

Lemma B.3. $EI_{t-1}(\mathbf{x})$ satisfies $EI_{t-1}(\mathbf{x}) \geq 0$ and $EI_{t-1}(\mathbf{x}) \geq f_{t-1}^+ - \mu_{t-1}(\mathbf{x})$. Moreover,

$$z_{t-1}(\mathbf{x}) \leq \frac{EI_{t-1}(\mathbf{x})}{\sigma_{t-1}(\mathbf{x})} = \tau(z_{t-1}(\mathbf{x})) < \begin{cases} \phi(z_{t-1}(\mathbf{x})), & z_{t-1}(\mathbf{x}) < 0 \\ z_{t-1}(\mathbf{x}) + \phi(z_{t-1}(\mathbf{x})), & z_{t-1}(\mathbf{x}) \geq 0. \end{cases} \quad (30)$$

Proof. From the definition of I_{t-1} and EI_{t-1} , the first statement follows immediately. By (5),

$$\frac{EI_{t-1}(\mathbf{x})}{\sigma_{t-1}(\mathbf{x})} = z_{t-1}(\mathbf{x})\Phi(z_{t-1}(\mathbf{x})) + \phi(z_{t-1}(\mathbf{x})). \quad (31)$$

If $z_{t-1}(\mathbf{x}) < 0$, or equivalently $f_{t-1}^+ - \mu_{t-1}(\mathbf{x}) < 0$, (31) leads to $\frac{EI_{t-1}(\mathbf{x})}{\sigma_{t-1}(\mathbf{x})} < \phi(z_{t-1}(\mathbf{x}))$. If $z_{t-1}(\mathbf{x}) \geq 0$, $\Phi(\cdot) < 1$ gives us $\frac{EI_{t-1}(\mathbf{x})}{\sigma_{t-1}(\mathbf{x})} < z_{t-1}(\mathbf{x}) + \phi(z_{t-1}(\mathbf{x}))$. The left inequality in (30) is an immediate result of $EI_{t-1}(\mathbf{x}) \geq f_{t-1}^+ - \mu_{t-1}(\mathbf{x})$. \square

The monotonicity of the exploration and exploitation of (17) is given next, previously also shown in [23].

Lemma B.4. $EI(a, b)$ is monotonically increasing in both a and b for $b \in (0, 1]$.

Proof. We prove the lemma by taking the derivative of $EI(a, b)$ with respect to both variables. First,

$$\frac{\partial EI(a, b)}{\partial a} = \Phi\left(\frac{a}{b}\right) + a\phi\left(\frac{a}{b}\right)\frac{1}{b} + b\frac{\partial\phi\left(\frac{a}{b}\right)}{\partial a}. \quad (32)$$

From (21), (32) is

$$\frac{\partial EI(a, b)}{\partial a} = \Phi\left(\frac{a}{b}\right) + \phi\left(\frac{a}{b}\right)\frac{a}{b} - \phi\left(\frac{a}{b}\right)\frac{a}{b} = \Phi\left(\frac{a}{b}\right) > 0. \quad (33)$$

Similarly,

$$\frac{\partial EI(a, b)}{\partial b} = -a\phi\left(\frac{a}{b}\right)\frac{a}{b^2} + \phi\left(\frac{a}{b}\right) - b\phi\left(\frac{a}{b}\right)\frac{a}{b}\left(-\frac{a}{b^2}\right) = \phi\left(\frac{a}{b}\right) > 0. \quad (34)$$

\square

The next lemma puts a lower bound on $f_{t-1}^+ - \mu_{t-1}(\mathbf{x}) < 0$ if $EI_{t-1}(\mathbf{x})$ is bounded below by a positive sequence denoted as κ_t . It is also previously shown in [32].

Lemma B.5. If $EI_{t-1}(\mathbf{x}) \geq \kappa_t$ for some $\kappa_t \in (0, \frac{1}{\sqrt{2\pi}})$ and $f_{t-1}^+ - \mu_{t-1}(\mathbf{x}) < 0$, then we have

$$f_{t-1}^+ - \mu_{t-1}(\mathbf{x}) \geq -\sqrt{2\log\left(\frac{1}{\sqrt{2\pi}\kappa_t}\right)}\sigma_{t-1}(\mathbf{x}). \quad (35)$$

Proof. By definition of $EI_{t-1}(\mathbf{x})$,

$$\begin{aligned} \kappa_t &\leq (f_{t-1}^+ - \mu_{t-1}(\mathbf{x}))\Phi(z_{t-1}(\mathbf{x})) + \sigma_{t-1}(\mathbf{x})\phi(z_{t-1}(\mathbf{x})) < \sigma_{t-1}(\mathbf{x})\phi(z_{t-1}(\mathbf{x})) \\ &= \sigma_{t-1}(\mathbf{x})\frac{1}{\sqrt{2\pi}}e^{-\frac{1}{2}z_{t-1}^2(\mathbf{x})} \leq \frac{1}{\sqrt{2\pi}}e^{-\frac{1}{2}z_{t-1}^2(\mathbf{x})}. \end{aligned} \quad (36)$$

Rearranging and taking the logarithm of (36), we have

$$2\log\left(\frac{1}{\sqrt{2\pi}\kappa_t}\right) > z_{t-1}^2(\mathbf{x}) = \left(\frac{f_{t-1}^+ - \mu_{t-1}(\mathbf{x})}{\sigma_{t-1}(\mathbf{x})}\right)^2. \quad (37)$$

Given that $f_{t-1}^+ - \mu_{t-1}(\mathbf{x}) < 0$, we recover (35). \square

A global lower bound of the posterior variance is given in the next lemma.

Lemma B.6. *The posterior standard deviation (2) has the lower bound*

$$\sigma_t(\mathbf{x}) \geq \sqrt{\frac{\epsilon}{t+\epsilon}}. \quad (38)$$

Proof. We invoke the fact that the minimum posterior standard deviation at \mathbf{x} is obtained if the previous t samples are all \mathbf{x} . In this case, all entries of \mathbf{K}_t are 1. It is easy to verify that

$$(\mathbf{K}_t + \epsilon \mathbf{I})^{-1} = -\frac{1}{t\epsilon + \epsilon^2} \mathbf{P} + \frac{1}{\epsilon} \mathbf{I}, \quad (39)$$

where \mathbf{P} is a $t \times t$ matrix with all entries being 1. Thus, by (2), we have

$$\sigma_t^2(\mathbf{x}) \geq 1 - \mathbf{p}^T \left[-\frac{1}{t+\epsilon} \mathbf{P} + \frac{1}{\epsilon} \mathbf{I} \right] \mathbf{p} = \frac{\epsilon}{t+\epsilon}, \quad (40)$$

where \mathbf{p} is the t -dimensional vector with all 1 entries. \square

Next, we present a well-established bound on f and the prediction $\mu_{t-1}(\mathbf{x})$.

Lemma B.7. *For any given $\mathbf{x} \in C$ and $t \geq 1$,*

$$|f(\mathbf{x}) - \mu_{t-1}(\mathbf{x})| \leq B\sigma_{t-1}(\mathbf{x}). \quad (41)$$

The proof of Lemma B.7 can be found in Theorem 2 of [9]. Next, we extend the bounds to $|I_{t-1}(\mathbf{x}) - EI_{t-1}(\mathbf{x})|$. An upper bound of $I_{t-1}(\mathbf{x}) - EI_{t-1}(\mathbf{x})$ is given in the next lemma.

Lemma B.8. *For any given $\mathbf{x} \in C$, $t \in \mathbb{N}$, and $w > 0$,*

$$I_{t-1}(\mathbf{x}) - EI_{t-1}(\mathbf{x}) < \begin{cases} \sigma_t(\mathbf{x})w, & f_{t-1}^+ - f(\mathbf{x}) \leq 0 \\ -f(\mathbf{x}) + \mu_{t-1}(\mathbf{x}), & f_{t-1}^+ - f(\mathbf{x}) > 0. \end{cases} \quad (42)$$

Proof. If $f_{t-1}^+ - f(\mathbf{x}) \leq 0$, we have by definition (4) and Lemma B.3,

$$I_{t-1}(\mathbf{x}) - EI_{t-1}(\mathbf{x}) = -EI_{t-1}(\mathbf{x}) < 0 < \sigma_{t-1}(\mathbf{x})w. \quad (43)$$

For $f_{t-1}^+ - f(\mathbf{x}) > 0$, we can write via Lemma B.3,

$$\begin{aligned} I_{t-1}(\mathbf{x}) - EI_{t-1}(\mathbf{x}) &= f_{t-1}^+ - f(\mathbf{x}) - EI_{t-1}(\mathbf{x}) \\ &\leq f_{t-1}^+ - f(\mathbf{x}) - f_{t-1}^+ + \mu_{t-1}(\mathbf{x}) < -f(\mathbf{x}) + \mu_{t-1}(\mathbf{x}). \end{aligned} \quad (44)$$

\square

An upper bound on $I_{t-1}(\mathbf{x})$ and $EI_{t-1}(\mathbf{x})$ is given in the next lemma.

Lemma B.9. *The improvement function and EI function satisfy*

$$I_{t-1}(\mathbf{x}) \leq \frac{\tau(B)}{\tau(-B)} EI_{t-1}(\mathbf{x}), \forall \mathbf{x} \in C, \forall t \in \mathbb{N}. \quad (45)$$

Proof. We consider two cases. First, if $f_{t-1}^+ - f(\mathbf{x}) \leq 0$, then $I_{t-1}(\mathbf{x}) = 0$. Since $EI_{t-1}(\mathbf{x}) \geq 0$, (45) stands.

Second, if $f_{t-1}^+ - f(\mathbf{x}) > 0$, then

$$f_{t-1}^+ - \mu_{t-1}(\mathbf{x}) = f_{t-1}^+ - f(\mathbf{x}) + f(\mathbf{x}) - \mu_{t-1}(\mathbf{x}) > f(\mathbf{x}) - \mu_{t-1}(\mathbf{x}). \quad (46)$$

From the one-side inequality in Lemma B.7, (46) implies

$$f_{t-1}^+ - \mu_{t-1}(\mathbf{x}) > -B\sigma_{t-1}(\mathbf{x}). \quad (47)$$

Then, from Lemma B.1 the monotonicity of $\tau(\cdot)$, we have

$$\tau(z_{t-1}(\mathbf{x})) > \tau(-B), \quad (48)$$

where $z_{t-1}(\mathbf{x}) = \frac{f_{t-1}^+ - \mu_{t-1}(\mathbf{x})}{\sigma_{t-1}(\mathbf{x})}$. Since $EI_{t-1}(\mathbf{x}) = \sigma_{t-1}(\mathbf{x})\tau(z_{t-1}(\mathbf{x}))$, we can write

$$EI_{t-1}(\mathbf{x}) = \sigma_{t-1}(\mathbf{x})\tau(z_{t-1}(\mathbf{x})) > \tau(-B)\sigma_{t-1}(\mathbf{x}). \quad (49)$$

Next, we let $w = B$ in Lemma B.8 and obtain

$$I_{t-1}(\mathbf{x}) - EI_{t-1}(\mathbf{x}) \leq -f(\mathbf{x}) + \mu_{t-1}(\mathbf{x}) \leq B\sigma_{t-1}(\mathbf{x}). \quad (50)$$

Applying (50) to (49) by eliminating $\sigma_{t-1}(\mathbf{x})$ and using union bound, we have

$$EI_{t-1}(\mathbf{x}) > \frac{\tau(-B)}{B + \tau(-B)}I_{t-1}(\mathbf{x}) = \frac{\tau(-B)}{\tau(B)}I_{t-1}(\mathbf{x}). \quad (51)$$

□

A similar result to Lemma B.9 is previously shown in [7].

C Instantaneous Regret Bound Proof

Proof of Lemma 3.2 is given next.

Proof. We consider two cases based on the value of $f_{t-1}^+ - f(\mathbf{x}_t)$. First, $f_{t-1}^+ \leq f(\mathbf{x}_t)$. From Lemma B.7 and B.9,

$$\begin{aligned} r_t &= f(\mathbf{x}_t) - f(\mathbf{x}^*) = f(\mathbf{x}_t) - f_{t-1}^+ + f_{t-1}^+ - f(\mathbf{x}^*) \leq f(\mathbf{x}_t) - f_{t-1}^+ + I_{t-1}(\mathbf{x}^*) \\ &\leq f(\mathbf{x}_t) - \mu_{t-1}(\mathbf{x}_t) + \mu_{t-1}(\mathbf{x}_t) - f_{t-1}^+ + \frac{\tau(B)}{\tau(-B)}EI_{t-1}(\mathbf{x}^*) \\ &\leq \mu_{t-1}(\mathbf{x}_t) - f_{t-1}^+ + c_B EI_{t-1}(\mathbf{x}_t) + B\sigma_{t-1}(\mathbf{x}_t), \end{aligned} \quad (52)$$

where $c_B = \frac{\tau(B)}{\tau(-B)}$.

Next, we aim to provide a lower bound for $EI_{t-1}(\mathbf{x}_t)$ by comparing $EI_{t-1}(\mathbf{x}_t)$ to $EI_{t-1}(\mathbf{x}^*)$. For $EI_{t-1}(\mathbf{x}^*)$, we can write via Lemma B.7 that

$$\begin{aligned} EI_{t-1}(\mathbf{x}^*) &= \sigma_{t-1}(\mathbf{x}^*)\tau(z_{t-1}(\mathbf{x}^*)) = \sigma_{t-1}(\mathbf{x}^*)\tau\left(\frac{f_{t-1}^+ - f(\mathbf{x}^*) + f(\mathbf{x}^*) - \mu_{t-1}(\mathbf{x}^*)}{\sigma_{t-1}(\mathbf{x}^*)}\right) \\ &\geq \sigma_{t-1}(\mathbf{x}^*)\tau\left(\frac{f_{t-1}^+ - f(\mathbf{x}^*)}{\sigma_{t-1}(\mathbf{x}^*)} - B\right) \geq \sigma_{t-1}(\mathbf{x}^*)\tau(-B), \end{aligned} \quad (53)$$

where the second inequality uses $f(\mathbf{x}^*) \leq f(\mathbf{x})$. By definition $EI_{t-1}(\mathbf{x}_t) \geq EI_{t-1}(\mathbf{x}^*)$. By Lemma B.6, (53) implies

$$EI_{t-1}(\mathbf{x}_t) \geq \tau(-B)\sqrt{\frac{\epsilon}{t + \epsilon}}. \quad (54)$$

It is easy to see that $\tau(-B)\sqrt{\frac{\epsilon}{t + \epsilon}} < \frac{1}{\sqrt{2\pi}}$. By Lemma B.5, (54) implies

$$f_{t-1}^+ - \mu_{t-1}(\mathbf{x}_t) \geq -\log^{\frac{1}{2}}\left(\frac{t + \epsilon}{2\pi\tau^2(-B)\epsilon}\right)\sigma_{t-1}(\mathbf{x}_t). \quad (55)$$

Equivalently,

$$\mu_{t-1}(\mathbf{x}_t) - f_{t-1}^+ \leq c_{B\epsilon}(\epsilon, t)\sigma_{t-1}(\mathbf{x}_t). \quad (56)$$

where $c_{B\epsilon}(\epsilon, t) = \log^{\frac{1}{2}}\left(\frac{t+\epsilon}{2\pi\tau^2(-B)\epsilon}\right)$. Using Lemma B.7, $\Phi(\cdot) < 1$, and $f_{t-1}^+ - f(\mathbf{x}_t) \leq 0$, we have

$$\begin{aligned} EI_{t-1}(\mathbf{x}_t) &= (f_{t-1}^+ - \mu_{t-1}(\mathbf{x}_t))\Phi(z_{t-1}(\mathbf{x}_t)) + \sigma_{t-1}(\mathbf{x}_t)\phi(z_{t-1}(\mathbf{x}_t)) \\ &\leq (f_{t-1}^+ - f(\mathbf{x}_t) + f(\mathbf{x}_t) - \mu_{t-1}(\mathbf{x}_t))\Phi(z_{t-1}(\mathbf{x}_t)) + \phi(0)\sigma_{t-1}(\mathbf{x}_t) \\ &\leq B\sigma_{t-1}(\mathbf{x}_t) + \phi(0)\sigma_{t-1}(\mathbf{x}_t). \end{aligned} \quad (57)$$

Applying (57) and (56) to (52), we have

$$r_t \leq (c_{B\epsilon}(\epsilon, t) + B + c_B(B + \phi(0)))\sigma_{t-1}(\mathbf{x}_t). \quad (58)$$

Second, if $f_{t-1}^+ - f(\mathbf{x}_t) \geq 0$, we have

$$\begin{aligned} r_t &= f(\mathbf{x}_t) - f(\mathbf{x}^*) = f(\mathbf{x}_t) - f_{t-1}^+ + f_{t-1}^+ - f(\mathbf{x}^*) \\ &\leq f(\mathbf{x}_t) - f_{t-1}^+ + c_B EI_{t-1}(\mathbf{x}^*) \\ &\leq f(\mathbf{x}_t) - f_{t-1}^+ + c_B EI_{t-1}(\mathbf{x}_t). \end{aligned} \quad (59)$$

The first inequality in (59) is by Lemma B.9. Further, we can write

$$\begin{aligned} EI_{t-1}(\mathbf{x}_t) &= (f_{t-1}^+ - \mu_{t-1}(\mathbf{x}_t))\Phi(z_{t-1}(\mathbf{x}_t)) + \sigma_{t-1}(\mathbf{x}_t)\phi(z_{t-1}(\mathbf{x}_t)) \\ &\leq (f_{t-1}^+ - f(\mathbf{x}_t) + f(\mathbf{x}_t) - \mu_{t-1}(\mathbf{x}_t))\Phi(z_{t-1}(\mathbf{x}_t)) + \phi(0)\sigma_{t-1}(\mathbf{x}_t) \\ &\leq f_{t-1}^+ - f(\mathbf{x}_t) + B\sigma_{t-1}(\mathbf{x}_t) + \phi(0)\sigma_{t-1}(\mathbf{x}_t). \end{aligned} \quad (60)$$

Applying (60) to (59), we have

$$r_t \leq (c_B - 1)(f_{t-1}^+ - f(\mathbf{x}_t)) + c_B(B + \phi(0))\sigma_{t-1}(\mathbf{x}_t). \quad (61)$$

Combine (58) and (61) and we have

$$r_t \leq \max\{c_B - 1, 0\} \max\{f_{t-1}^+ - f(\mathbf{x}_t), 0\} + (c_{B\epsilon}(\epsilon, t) + B + c_B(B + \phi(0)))\sigma_{t-1}(\mathbf{x}_t). \quad (62)$$

□

D Cumulative Regret Bound Proof

The proof of Lemma 3.5 is given next.

Proof. From Lemma 3.2, we consider the term $\sum_{t=1}^T \max\{f_{t-1}^+ - f(\mathbf{x}_t), 0\}$. Let $P_T \subseteq \{1, \dots, T\}$ be the ordered index set such that $f_{t-1}^+ - f(\mathbf{x}_t) > 0$. Then, using $t_i - 1 \geq t_{i-1}$, we have

$$\sum_{t=1}^T \max\{f_{t-1}^+ - f(\mathbf{x}_t), 0\} = \sum_{i=1}^{|P_T|} f_{t_i-1}^+ - f(\mathbf{x}_{t_i}) \leq \sum_{i=1}^{|P_T|} f(\mathbf{x}_{t_{i-1}}) - f(\mathbf{x}_{t_i}), \quad (63)$$

where $t_i \in P_T$ and $t_i < t_{i+1}$. Since $f_t^+ \leq f(\mathbf{x}_t)$ for $\forall t \in \mathbb{N}$, (63) leads to

$$\begin{aligned} \sum_{t=1}^T \max\{f_{t-1}^+ - f(\mathbf{x}_t), 0\} &\leq \sum_{i=1}^{|P_T|} f(\mathbf{x}_{t_{i-1}}) - f(\mathbf{x}_{t_i}) \\ &\leq (f_{t_0} - f_{t_{|P_T|}}) \leq 2B, \end{aligned} \quad (64)$$

where we used the boundedness of f in Lemma A.6. Using (64) in (10), we have

$$\begin{aligned} R_T &= \sum_{t=1}^T r_t \leq \sum_{t=1}^T c_{B1} \max\{f_{t-1}^+ - f(\mathbf{x}_t), 0\} + \sum_{t=1}^T (c_{B\epsilon}(T) + B + c_B(B + \phi(0)))\sigma_{t-1}(\mathbf{x}_t) \\ &\leq 2c_{B1}B + (c_{B\epsilon}(\epsilon, T) + B + c_B(B + \phi(0))) \sum_{t=1}^T \sigma_{t-1}(\mathbf{x}_t). \end{aligned} \quad (65)$$

□

Proof of Theorem 3.6 is given next.

Proof. From Lemma A.4, we know $\sum_{t=1}^T \sigma_{t-1}(\mathbf{x}_t) = \mathcal{O}(\sqrt{T\gamma_T})$. From Lemma 3.5, the cumulative regret bound is

$$\mathcal{O}(R_T) = \mathcal{O}(\log^{1/2}(T)\sqrt{T\gamma_T}). \quad (66)$$

Using $\gamma_T = \mathcal{O}(\log^{d+1}(T))$ for SE kernel, we have $R_T = \mathcal{O}(T^{1/2} \log^{\frac{d+2}{2}}(T))$. Using $\gamma_T = \mathcal{O}(T^{\frac{d}{2\nu+d}} \log^{\frac{2\nu}{2\nu+d}}(T))$ for Matérn kernel from [20, 46], we have $R_T = \mathcal{O}(T^{\frac{\nu+d}{2\nu+d}} \log^{\frac{2\nu+0.5d}{2\nu+d}}(T))$. \square

E Proof of Nugget Effect

The maximum information gain bounds are given below from [20]. We use the following lemma on the upper bound of γ_T .

Lemma E.1 (Maximum information gain upper bound, Theorem 7 in [20]). *Assume the domain satisfies $C = \{\mathbf{x} \in \mathbb{R}^d, \|\mathbf{x}\|_2 \leq 1\}$. At given d and T , for SE kernel, if $\theta \leq e^2 c_d$ and $T \geq (e-1)\epsilon$,*

$$\gamma_T(\epsilon) \leq \frac{C_d^1}{\theta^d} \log^{d+1}(1+T/\epsilon) + \log(1+T/\epsilon) + C_d^2 \exp\left(-\frac{2}{\theta} + \frac{1}{\theta^2}\right), \quad (67)$$

Further, for $\theta > e^2 c_d$,

$$\gamma_T(\epsilon) \leq \frac{C_d^3}{\log^d\left(\frac{\theta}{e c_d}\right)} \log^{d+1}\left(1 + \frac{T}{\epsilon}\right) + C_d^4 \log\left(1 + \frac{T}{\epsilon}\right) + C_d^5, \quad (68)$$

where $\theta = 2l^2$ and $c_d = \max\{1, \exp(\frac{1}{e}(\frac{d}{2} - 1))\}$. The constants $C_d^i, i = 1, \dots, 5$ only depend on d .

For Matérn kernels with smoothness $\nu > \frac{1}{2}$, we have

$$\gamma_T(\epsilon) \leq C(T, \nu, \epsilon) \bar{\gamma}_T + C, \quad (69)$$

where $C_\nu > 0$ only depends on ν , C is a constant, and

$$C(T, \nu, \lambda) = \max\left\{1, \log_2\left(1 + \frac{\Gamma(\nu)}{C_\nu} \log\left(\frac{T^2}{\epsilon}\right)\right) + \frac{1}{\nu} \log_2\left(\frac{T^2}{\nu \Gamma(\nu) \epsilon}\right) + 1\right\}, \quad (70)$$

Furthermore,

$$\bar{\gamma}_T(\epsilon) = C_{d,\nu}^1 \log\left(1 + \frac{2T}{\epsilon}\right) + C_{d,\nu}^2 \left(\frac{T}{\epsilon l^{2\nu}}\right)^{\frac{d}{2\nu+d}} \log^{\frac{2\nu}{2\nu+d}}\left(1 + \frac{2T}{\epsilon}\right). \quad (71)$$

The constants $C_{d,\nu}^i$ depend only on d and ν .

Given this premise, we rewrite Lemma E.1 into the following two lemmas on the bounds of γ_T .

Lemma E.2. *Assume the domain satisfies $C = \{\mathbf{x} \in \mathbb{R}^d, \|\mathbf{x}\|_2 \leq 1\}$. For a SE kernel with fixed l , there exist constants C_{dl}^1, C_{dl}^2 , and C_{dl}^3 such that*

$$\gamma_T(\epsilon) \leq s_T(\epsilon) = C_{dl}^1 \left[\log^{d+1}(1+T/\epsilon) + C_{dl}^2 \log(1+T/\epsilon) + C_{dl}^3 \right]. \quad (72)$$

where the constants depend only on given d and l .

Lemma E.3. *Assume the domain satisfies the condition in Theorem 7 in [1]. For a Matérn kernel with given $l, \nu > 1/2$ and d , suppose T/ϵ is large enough such that*

$$c_T^0(\epsilon) := C_\nu^1 [\log(1 + C_\nu^2 \log(T^2/\epsilon)) + C_\nu^3 \log(T^2/\epsilon) + C_\nu^4] \geq 1, \quad (73)$$

where $C_\nu^1 = \frac{1}{\log(2)}$, $C_\nu^2 = \frac{\Gamma(\nu)}{C_\nu}$, $C_\nu^3 = \frac{1}{\nu}$, $C_\nu^4 = \frac{1}{\nu} \log(\frac{1}{\nu\Gamma(\nu)}) + \log(2)$, $C_\nu > 0$ only depend on ν and Γ is the Gamma function. Notice that $C_\nu^i > 0, i = 1, \dots, 3$. Further, there exist $C_{d\nu l}^1$ and $C_{d\nu l}^2$ dependent only on d, ν and l so that

$$\bar{\gamma}_T(\epsilon) = C_{d\nu l}^1 [\log(1 + 2T/\epsilon) + C_{d\nu l}^2 (T\eta)^{\frac{d}{2\nu+d}} \log^{\frac{2\nu}{2\nu+d}}(1 + 2T/\epsilon)],$$

where $C_{d\nu l}^1 = C_{d,\nu}^{(1)}$ and $C_{d\nu l}^2 = (C_{d,\nu}^{(2)}(l)^{-2\nu d/(2\nu+d)})/(C_{d,\nu}^{(1)})$ (see [1] for constants $C_{d,\nu}^{(i)}, i = 1, 2$). Then, there exists constants $C > 0$ such that its γ_T satisfies

$$\gamma_T(\epsilon) \leq s_T(\epsilon) = c_T^0(\epsilon)\bar{\gamma}_T(\epsilon) + C.$$

Note that C_ν^4 is not necessarily positive. The assumption that $c_T^0(\epsilon) \geq 1$ can be achieved when $T/\epsilon \gg 1$. We shall further assume that T/ϵ is sufficiently large such that $c_T^0(\epsilon)\bar{\gamma}_T(\epsilon) \geq C$.

Next, we simplify the upper bound of $R_T(\epsilon)$.

Lemma E.4. Let $C_R^1 = 2c_{B1}B$, $C_R^2 = \log\left(\frac{1}{2\pi\tau^2(-B)}\right)$, $C_R^3 = B + c_B(B + \phi(0))$, and $C_R^4 = C_R^2 + (C_R^3)^2$ (see Lemma 3.5 for constants). Suppose the upper bound on $\gamma_T(\epsilon)$ is $\gamma_T(\epsilon) \leq s_T(\epsilon)$. Define

$$c_T(\epsilon) = \left(\log(1 + T/\epsilon) + 2C_R^3(\log(1 + T/\epsilon) + C_R^2)^{1/2} + C_R^4\right) \frac{1}{\log(1 + 1/\epsilon)} s_T(\epsilon),$$

Then, the cumulative regret upper bound from Lemma 3.5 is

$$R_T \leq C_R^1 + u_T(\epsilon), \text{ where } u_T(\epsilon) = \sqrt{2c_T(\epsilon)T} \quad (74)$$

Proof. By Lemma 3.5,

$$\begin{aligned} R_T &\leq 2c_{B1}B + (c_{B\epsilon}(\epsilon, T) + B + c_B(B + \phi(0)))\sqrt{C_\gamma(\epsilon)T\gamma_T(\epsilon)} \\ &\leq C_R^1 + (\sqrt{C_R^2 + \log(1 + T/\epsilon)} + C_R^3)\sqrt{C_\gamma(\epsilon)Ts_T(\epsilon)} \\ &= C_R^1 + \sqrt{c_T(\epsilon)}\sqrt{2T}. \end{aligned} \quad (75)$$

□

First, we present the proof for SE kernel. The proof of Theorem 4.2 is given below.

Proof. From Lemma E.4, at a given T , the upper bound on $R_T(\epsilon)$ changes the same way as $c_T(\epsilon)$. In particular, by Lemma E.2 we only need to consider $c_T(\epsilon)/C_{dl}^1$. Hence, in the following, we analyze how $c_T(\epsilon)$ changes with ϵ .

For simplicity, let $\eta = \frac{1}{\epsilon}$. We define the following shorthands for terms in $c_T(\eta)$:

$$c_T^1(\eta) = \log(1 + T\eta) + 2C_R^3(\log(1 + T\eta) + C_R^2)^{1/2} + C_R^4, \quad (76)$$

and

$$c_T^2(\eta) = \log^{d+1}(1 + T\eta) + C_{dl}^2 \log(1 + T\eta) + C_{dl}^3. \quad (77)$$

Thus, by Lemma E.2,

$$c_T(\eta)/C_{dl}^1 = c_T^1(\eta) \frac{1}{\log(1 + \eta)} c_T^2(\eta). \quad (78)$$

Define $c_T^3(\eta) := c_T^1(\eta)c_T^2(\eta)$. We expand it into the sum of nine terms:

$$\begin{aligned} &\log^{d+2}(1 + T\eta) + 2C_R^3(\log(1 + T\eta) + C_R^2)^{1/2} \log^{d+1}(1 + T\eta) + C_R^4 \log^{d+1}(1 + T\eta) + \\ &C_{dl}^2 \log^2(1 + T\eta) + 2C_R^3 C_{dl}^2 (\log(1 + T\eta) + C_R^2)^{1/2} \log(1 + T\eta) + C_R^4 C_{dl}^2 \log(1 + T\eta) + \\ &C_{dl}^3 \log(1 + T\eta) + 2C_R^3 C_{dl}^3 (\log(1 + T\eta) + C_R^2)^{1/2} + C_R^4 C_{dl}^3. \end{aligned} \quad (79)$$

By (78), differentiating $c_T(\eta)/C_{dl}^1$ gives

$$\frac{dc_T(\eta)}{d\eta} \frac{1}{C_{dl}^1} = \frac{1}{\log^2(1 + \eta)} \left[\log(1 + \eta) \frac{dc_T^3(\eta)}{d\eta} - \frac{1}{1 + \eta} c_T^3(\eta) \right]. \quad (80)$$

Thus, the sign of $\frac{dc_T(\eta)}{d\eta}$ is the sign of d_c defined as

$$d_c(\eta) := \log(1 + \eta) \frac{dc_T^3(\eta)}{d\eta} - \frac{1}{1 + \eta} c_T^3(\eta). \quad (81)$$

For simplicity, we suppress the dependence on the given T . Next, we expand $d_c(\eta)$ in (81) as the sum of nine terms, each corresponding to one term in (79). The first term is $\log^{d+2}(1 + T\eta)$ and its contribution to $d_c(\eta)$ is

$$d_c^1(\eta) := \log^{d+1}(1 + T\eta) \left[(d + 2) \frac{1}{1/T + \eta} \log(1 + \eta) - \frac{1}{1 + \eta} \log(1 + T\eta) \right]. \quad (82)$$

If (13) is satisfied, then

$$d_c^1(\eta) > \frac{1}{1 + \eta} \log^{d+1}(1 + T\eta) ((d + 2) \log(1 + \eta) - \log(1 + T\eta)) > \frac{1}{1 + \eta} \frac{1}{d + 1} \log^{d+2}(1 + T\eta). \quad (83)$$

Now we repeat this derivation for the second term. Its contribution to (81) is

$$d_c^2(\eta) := 2C_R^3 (\log(1 + T\eta) + C_R^2)^{1/2} \log^d(1 + T\eta) \left[(d + 1) \log(1 + \eta) \frac{1}{1/T + \eta} + \frac{1}{2(1/T + \eta)} \frac{\log(1 + \eta)}{1 + C_R^2/\log(1 + T\eta)} - \frac{1}{1 + \eta} \log(1 + T\eta) \right]. \quad (84)$$

If (13) is satisfied,

$$d_c^2(\eta) > 2C_R^3 (\log(1 + T\eta) + C_R^2)^{1/2} \log^d(1 + T\eta) \frac{1}{(1 + \eta)(2(d + 1))} \frac{\log(1 + T\eta)}{1 + C_R^2/\log(1 + T\eta)}. \quad (85)$$

The third term adds to (81) as

$$d_c^3(\eta) := C_R^4 \log^d(1 + T\eta) \left[(d + 1) \log(1 + \eta) \frac{1}{1/T + \eta} - \frac{\log(1 + T\eta)}{1 + \eta} \right]. \quad (86)$$

If (13) holds, then $d_c^3(\eta) > 0$. The fourth derivative is

$$d_c^4(\eta) := C_{dl}^2 \log(1 + T\eta) \left[2 \log(1 + \eta) \frac{1}{1/T + \eta} - \frac{\log(1 + T\eta)}{1 + \eta} \right]. \quad (87)$$

With (13), we can write

$$d_c^4(\eta) > -C_{dl}^2 \log^2(1 + T\eta) \frac{1}{1 + \eta} \frac{d - 1}{d + 1}. \quad (88)$$

For the fifth term, its role in (81) is

$$d_c^5(\eta) := 2C_R^3 C_{dl}^2 (\log(1 + T\eta) + C_R^2)^{1/2} \left[\log(1 + \eta) \frac{1}{1/T + \eta} + \frac{1}{2(1/T + \eta)} \frac{\log(1 + \eta)}{1 + C_R^2/\log(1 + T\eta)} - \frac{\log(1 + T\eta)}{1 + \eta} \right]. \quad (89)$$

Given (13),

$$d_c^5(\eta) > \frac{2C_R^3 C_{dl}^2}{1 + \eta} (\log(1 + T\eta) + C_R^2)^{1/2} \left[\frac{1}{2(d + 1)} \frac{\log(1 + T\eta)}{1 + C_R^2/\log(1 + T\eta)} - \frac{d}{d + 1} \log(1 + T\eta) \right]. \quad (90)$$

The sixth and seventh terms can be combined can yield for (81)

$$d_c^{67}(\eta) := (C_R^4 C_{dl}^2 + C_{dl}^3) \left[\log(1 + \eta) \frac{1}{1/T + \eta} - \frac{\log(1 + T\eta)}{(1 + \eta)} \right]. \quad (91)$$

By (13),

$$d_c^{67}(\eta) > -(C_R^4 C_{dl}^2 + C_{dl}^3) \frac{1}{1+\eta} \frac{d}{d+1} \log(1+T\eta). \quad (92)$$

The eighth term leads to

$$d_c^8(\eta) := 2C_R^3 C_{dl}^3 (\log(1+T\eta) + C_R^2)^{1/2} \left[\frac{1}{2(1/T + \eta)} \frac{\log(1+\eta)}{\log(1+T\eta) + C_R^2} - \frac{1}{1+\eta} \right]. \quad (93)$$

Using (13),

$$d_c^8(\eta) > 2C_R^3 C_{dl}^3 (\log(1+T\eta) + C_R^2)^{1/2} \frac{1}{\eta+1} \left[\frac{1}{2(d+1)} \frac{1}{1 + C_R^2/\log(1+T\eta)} - 1 \right]. \quad (94)$$

The last term leads to in (1)

$$d_c^9(\eta) := -C_R^4 C_{dl}^3 \frac{1}{1+\eta}. \quad (95)$$

Since $d_c(\eta) = \sum_{i=1}^9 d_c^i(\eta)$, we consider the order of the lower bound of $d_c^i(\eta)$ to find the sign of $d_c(\eta)$. Combine the lower bounds above and lift common multiplier $1/(1+\eta)$. Since $\log(1+T\eta) \gg 1$, we can write the order of each term as follows.

The order of the positive lower bounds are $\log^{d+2}(1+T\eta)$ (83) and $\frac{1}{d} C_R^3 \log^{d+1.5}(1+T\eta)$ (85). For negative lower bounds, we have $-C_{dl}^2 \frac{d-1}{d+1} \log^2(1+T\eta)$ (87), $-C_R^3 C_{dl}^2 \log^{1.5}(1+T\eta)$ (89), $-(C_R^4 C_{dl}^2 + C_{dl}^3) \log(1+T\eta)$ (92), $-C_R^3 C_{dl}^3 \log^{0.5}(1+T\eta)$ (94), and $-C_R^4 C_{dl}^3$ (95). It is easy to verify that, for $d \geq 2$,

$$\frac{1}{d} C_R^3 \log^{d+1.5}(1+T\eta) \gg C_R^3 C_{dl}^2 \log^{1.5}(1+T\eta).$$

Further, using the positive bound from (83) satisfies

$$\begin{aligned} \log^{d+2}(1+T\eta) &\gg C_{dl}^2 \frac{d-1}{d+1} \log^2(1+T\eta), \\ \log^{d+2}(1+T\eta) &\gg (C_R^4 C_{dl}^2 + C_{dl}^3) \log(1+T\eta), \\ \log^{d+2}(1+T\eta) &\gg C_R^3 C_{dl}^3 \log^{0.5}(1+T\eta), \\ \log^{d+2}(1+T\eta) &\gg C_R^4 C_{dl}^3. \end{aligned} \quad (96)$$

Thus, by (80) and (81), we arrive at $d_c(\eta) > 0$ and $\frac{dc_T(\eta)}{\eta} > 0$. When $d = 1$, the conclusion remains the same as $d_c^4(\eta) > 0$, where $d_c^3(\eta)$ and $d_c^4(\eta)$ coincide.

Next, we consider if (14) is true. From $d_c^1(\eta)$ (82) and (14), we have $d_c^1(\eta) < 0$. Indeed, it is easy to verify that all $d_c^i(\eta) < 0, i = 2, \dots, 9$. Hence, $d_c < 0$ and $\frac{dc_T(\eta)}{\eta} < 0$. \square

The proof of Theorem 4.3 is given below.

Proof. Recall that from Lemma E.3 that $s_T(\epsilon) = c_T^0(\epsilon) \bar{\gamma}_T(\epsilon) + C$. By Lemma E.4, the cumulative regret bound changes the same way as $c_T(\epsilon)/(C_{dl}^1 C_\nu^1)$. First, define

$$\begin{aligned} c_T^1(\eta) &:= \log(1+T\eta) + 2C_R^3 (\log(1+T\eta) + C_R^2)^{1/2} + C_R^4, \\ c_T^2(\eta) &:= c_T^0(\eta)/C_\nu^1 = [\log(1+C_\nu^2 \log(T^2\eta)) + C_\nu^3 \log(T^2\eta) + C_\nu^4], \\ c_T^3(\eta) &:= \bar{\gamma}_T(\eta)/C_{dl}^1 = [\log(1+2T\eta) + C_{dl}^2 (T\eta)^{\frac{d}{2\nu+d}} \log^{\frac{2\nu}{2\nu+d}}(1+2T\eta)]. \end{aligned} \quad (97)$$

Let $c_T^{123}(\eta) = c_T^1(\eta) c_T^2(\eta) c_T^3(\eta)$. By Lemma E.3, we have

$$c_T(\eta) = C_\nu^1 C_{dl}^1 c_T^{123}(\eta) \frac{1}{\log(1+\eta)} + c_T^1(\eta) \frac{1}{\log(1+\eta)} C. \quad (98)$$

Consider the first part of (98). Its derivative is

$$C_\nu^1 C_{d\nu}^1 \frac{1}{\log^2(1+\eta)} \left[\log(1+\eta) \frac{dc_T^{123}(\eta)}{d\eta} - \frac{1}{1+\eta} c_T^{123}(\eta) \right]. \quad (99)$$

The sign of (99) is the same as the sign of

$$d_c(\eta) := \frac{dc_T^{123}(\eta)}{d\eta} \log(1+\eta) - \frac{1}{1+\eta} c_T^{123}(\eta). \quad (100)$$

Consider case (1) first. Since $c_T^i(\eta) > 0$ and increases with η , $i = 1, 2, 3$, we have

$$\begin{aligned} \frac{dc_T^{123}(\eta)}{d\eta} &= \frac{dc_T^1(\eta)}{d\eta} c_T^2(\eta) c_T^3(\eta) + \frac{dc_T^2(\eta)}{d\eta} c_T^1(\eta) c_T^3(\eta) + \frac{dc_T^3(\eta)}{d\eta} c_T^1(\eta) c_T^2(\eta) \\ &> \frac{dc_T^3(\eta)}{d\eta} c_T^1(\eta) c_T^2(\eta). \end{aligned} \quad (101)$$

The first two terms in the first equality above will be used later. Using (100) in (101), we have the lower bound

$$d_c(\eta) > c_T^1(\eta) c_T^2(\eta) \left[\frac{dc_T^3(\eta)}{d\eta} \log(1+\eta) - \frac{1}{1+\eta} c_T^3(\eta) \right]. \quad (102)$$

The derivative is

$$\begin{aligned} \frac{dc_T^3(\eta)}{d\eta} &= \frac{1}{\eta + 1/2T} + C_{d\nu}^2 \frac{d}{2\nu + d} (T\eta)^{\frac{d}{2\nu+d}} \frac{1}{\eta} \log^{\frac{2\nu}{2\nu+d}}(1 + 2T\eta) + \\ &C_{d\nu}^2 (T\eta)^{\frac{d}{2\nu+d}} \frac{2\nu}{2\nu + d} \log^{-\frac{d}{2\nu+d}}(1 + 2T\eta) \frac{1}{\eta + 1/2T}. \end{aligned} \quad (103)$$

Note that the first and third terms in (103) > 0 . By relaxing them and using (103) in (102), we have

$$\begin{aligned} d_c(\eta) &> c_T^1(\eta) c_T^2(\eta) C_{d\nu}^2 (T\eta)^{\frac{d}{2\nu+d}} \log^{\frac{2\nu}{2\nu+d}}(1 + 2T\eta) \frac{1}{1+\eta} \left[\frac{d}{2\nu + d} \log(1+\eta) \right. \\ &\quad \left. - \left(\frac{1}{C_{d\nu}^2} \left(\frac{\log(1 + 2T\eta)}{T\eta} \right)^{\frac{d}{2\nu+d}} + 1 \right) \right]. \end{aligned} \quad (104)$$

Since $\frac{\log(1+2T\eta)}{T\eta} < 1$ for $T\eta \gg 1$, from (15), we have

$$d_c(\eta) > c_T^1(\eta) c_T^2(\eta) C_{d\nu}^2 (T\eta)^{\frac{d}{2\nu+d}} \log^{\frac{2\nu}{2\nu+d}}(1 + 2T\eta) \frac{1}{1+\eta} \left[\frac{d \log(1+\eta)}{2\nu + d} - (1/C_{d\nu}^2 + 1) \right] > 0. \quad (105)$$

Next, we consider the second part in (98). Its derivative is

$$\frac{C}{\log^2(1+\eta)} \left[\log(1+\eta) \frac{dc_T^1(\eta)}{d\eta} - \frac{1}{1+\eta} c_T^1(\eta) \right]. \quad (106)$$

Given (15), we know the second term in (101) leads to

$$C_\nu^1 C_{d\nu}^1 \frac{dc_T^2(\eta)}{d\eta} c_T^1(\eta) c_T^3(\eta) \log(1+\eta) > C_\nu^1 C_{d\nu}^1 C_\nu^3 \frac{1}{\eta} c_T^1(\eta) \log(1 + 2T\eta) \log(1+\eta) > c_T^1(\eta) \frac{C}{1+\eta}. \quad (107)$$

Hence, by (99), (105), (98) and (107), we have $\frac{dc_T(\eta)}{d\eta} > 0$.

Next, we consider case 2. We use a more compact proof procedure given that $c_T^{123}(\eta)$ has 18 terms. Define $c_T^{13}(\eta) := c_T^1(\eta) c_T^3(\eta) = \sum_{p=1}^3 \sum_{q=1}^2 a_p^1(\eta) a_q^3(\eta)$, where

$$\begin{aligned} a_1^1(\eta) &= \log(1 + T\eta), a_2^1(\eta) = 2C_R^3(\log(1 + T\eta) + C_R^2)^{1/2}, a_3^1(\eta) = C_R^4, \\ a_1^3(\eta) &= \log(1 + 2T\eta), a_2^3(\eta) = C_{d\nu}^2 (T\eta)^{\frac{d}{2\nu+d}} \log^{\frac{2\nu}{2\nu+d}}(1 + 2T\eta). \end{aligned} \quad (108)$$

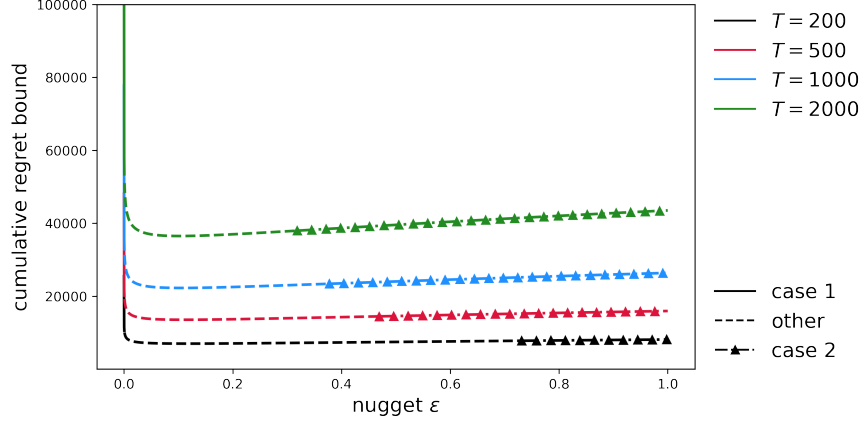


Figure 4: Cumulative regret upper bound with nugget ϵ at different T and selected constants for Matérn kernel ($\nu = \frac{1}{2}$). The case “other” means neither the conditions for case 1 nor those for case 2 are satisfied.

Thus, $d_c(\eta)$ can be written as

$$d_c(\eta) = \sum_{p=1}^3 \sum_{q=1}^2 c_T^2(\eta) a_p^1(\eta) a_q^3(\eta) \left[\left(\frac{da_p^1(\eta)}{d\eta} / a_p^1(\eta) + \frac{da_q^3(\eta)}{d\eta} / a_q^3(\eta) + \frac{dc_T^2(\eta)}{d\eta} / c_T^2(\eta) \right) \log(1 + \eta) - \frac{1}{1 + \eta} \right]. \quad (109)$$

We note that $c_T^2(\eta)$ is not decomposed for a even more compact proof because it is possible that $C_\nu^4 < 0$. Since $a_p^1(\eta), a_q^3(\eta), c_T^2(\eta) > 0$, to show $d_c(\eta) < 0$, it is sufficient to find the largest value of

$$d_{pq\eta} := \left[\frac{da_p^1(\eta)}{d\eta} / a_p^1(\eta) + \frac{da_q^3(\eta)}{d\eta} / a_q^3(\eta) + \frac{dc_T^2(\eta)}{d\eta} / c_T^2(\eta) \right] \log(1 + \eta) - \frac{1}{1 + \eta}, \quad (110)$$

for all p and q , a total of six terms, and show that it is < 0 . If this largest term generates $d_{pq\eta} < 0$, then the other five p, q combinations must also have $d_{pq\eta} < 0$ and, hence, the sum (109) will be < 0 . Using elementary algebra one can compare the six terms and verify that the largest $d_{pq\eta}(\eta)$ occurs at $p = 1$ and $q = 2$ given $T\eta \gg 1$. The third term in (110) is:

$$\frac{dc_T^2(\eta)}{d\eta} / c_T^2(\eta) < \frac{1}{\eta} \frac{1}{1/C_\nu^2 + \log(T^2\eta)} + C_\nu^3 < \frac{1}{\eta} \frac{1}{c_T^2(\eta)} \left(\frac{1}{\log(T^2\eta)} + C_\nu^3 \right). \quad (111)$$

Further,

$$\frac{da_1^1(\eta)}{d\eta} / a_1^1(\eta) = \frac{1}{1/T + \eta} \frac{1}{\log(1 + T\eta)}, \quad \frac{da_2^3(\eta)}{d\eta} / a_2^3(\eta) < \frac{1}{\eta} \left[\frac{d}{2\nu + d} + \frac{2\nu}{2\nu + d} \frac{1}{\log(1 + 2T\eta)} \right]. \quad (112)$$

Thus, for any p, q , we can write

$$\begin{aligned} d_{pq\eta} &< \frac{1}{\eta} \left[\frac{1}{\log(T\eta)} + \frac{d}{2\nu + d} + \frac{2\nu}{2\nu + d} \frac{1}{\log(2T\eta)} + \frac{1}{c_T^2(\eta)} \frac{1}{\log(T^2\eta)} + \frac{1}{c_T^2(\eta)} C_\nu^3 \right] \log(1 + \eta) - \frac{1}{1 + \eta} \\ &< \frac{1}{\eta} \left[\frac{d}{2\nu + d} + \frac{1}{\log(T\eta)} \left(\frac{4\nu + d}{2\nu + d} + \frac{1}{c_T^2(\eta)} \right) + \frac{C_\nu^3}{c_T^2(\eta)} \right] \log(1 + \eta) - \frac{1}{1 + \eta}, \end{aligned} \quad (113)$$

where we use $\log(T^2\eta) \geq \log(T\eta)$. By (16), (113) < 0 . Thus, the other five (smaller) terms in (110) are also < 0 . Thus, $d_c < 0$ by (109). Further, under (16), it is easy to verify that the second part in (98) < 0 and thus $\frac{dc_T(\eta)}{d\eta} < 0$. By Lemma E.4, the cumulative regret bound changes the same as c_T with respect to $\epsilon = 1/\eta$. \square

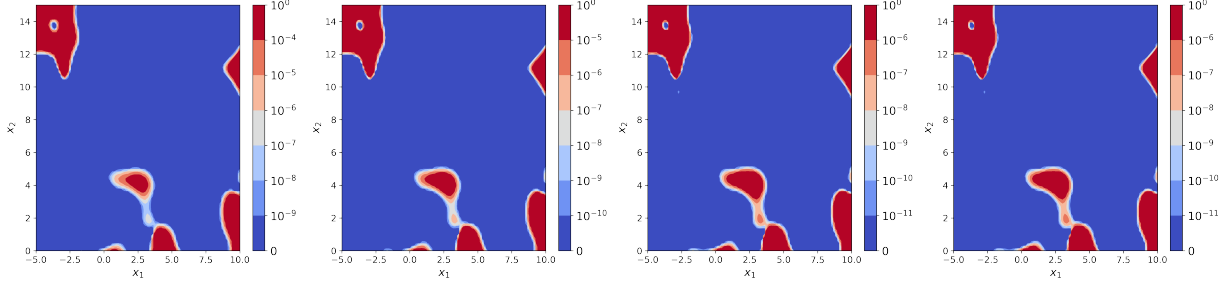


Figure 5: Illustrative example of EI contour of the Branin function with 50 random samples. From left to right: contour plots for $\epsilon = 10^{-2}$, $\epsilon = 10^{-6}$, $\epsilon = 10^{-10}$, and no nugget. The maximum EI_{50} value from left to right: 0.40515, 0.40085, 0.40085, and 0.40085. The maximum level of the colorbar corresponds to the maximum of EI_{50} of each plot.

F Numerical Example and Additional Plots

F.1 Plot for the Nugget Effect

As mentioned in Section 4, we choose the 50 samples entirely through random sampling for the Branin function and plot the EI contour using different nugget values in Figure 5. The effect of ϵ on the values of EI is much less obvious here, as expected.

F.2 Numerical Example Setup

The mathematical expression for example 1, the two-dimensional Rosenbrock function, is given below.

$$f(\mathbf{x}) = \sum_{i=1}^{d-1} [100(x_{i+1} - x_i^2)^2 + (x_i - 1)^2] \quad (114)$$

$$x_i \in [-2.048, 2.0480]^2.$$

The optimal objective function value is 0.

The mathematical expression for example 2, the six-hump camel function given below.

$$f(\mathbf{x}) = \left(4 - 2.1x_1^2 + \frac{x_1^4}{3}\right)x_1^2 + x_1x_2 + (-4 + 4x_2^2)x_2^2 \quad (115)$$

$$-3 \leq x_1 \leq 3, \quad -2 \leq x_2 \leq 2.$$

The optimal objective function value is -1.0316 .

The mathematical expression for example 3, the Hartmann6 function is given below.

$$f(\mathbf{x}) = - \sum_{i=1}^4 \alpha_i \exp \left(- \sum_{j=1}^6 A_{ij} (x_j - P_{ij})^2 \right) \quad (116)$$

$$x_i \in [0, 1], i = 1, \dots, 6$$

$$\alpha = [1.0, 1.2, 3.0, 3.2]^\top$$

$$A = \begin{bmatrix} 10 & 3.0 & 17 & 3.5 & 1.7 & 8.0 \\ 0.05 & 10 & 17 & 0.1 & 8.0 & 14 \\ 3.0 & 3.5 & 1.7 & 10 & 17 & 8.0 \\ 17 & 8.0 & 0.05 & 10 & 0.1 & 14 \end{bmatrix}$$

$$P = \begin{bmatrix} 0.131 & 0.170 & 0.557 & 0.012 & 0.828 & 0.587 \\ 0.233 & 0.414 & 0.831 & 0.374 & 0.100 & 0.999 \\ 0.235 & 0.145 & 0.352 & 0.288 & 0.305 & 0.665 \\ 0.405 & 0.883 & 0.873 & 0.574 & 0.109 & 0.038 \end{bmatrix}.$$

The optimal objective function value is -3.32 .

The mathematical expression for example 4, the Branin function, is given below.

$$f(\mathbf{x}) = \left(x_2 - \frac{5.1}{4\pi^2} x_1^2 + \frac{5}{\pi} x_1 - 6 \right)^2 + 10 \left(1 - \frac{1}{8\pi} \right) \cos(x_1) + 10 \quad (117)$$
$$x_1 \in [-5, 10], x_2 \in [0, 15].$$

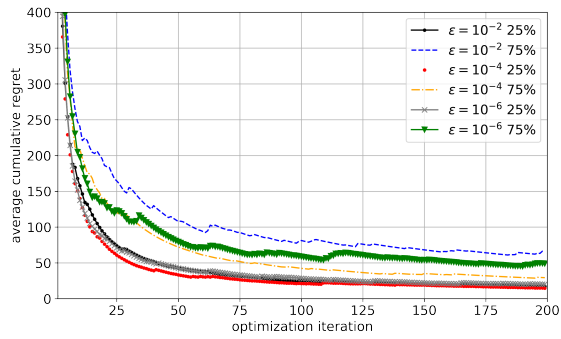
The optimal objective function value is 0 .

The mathematical expression for example 5, the Michalewicz function given below.

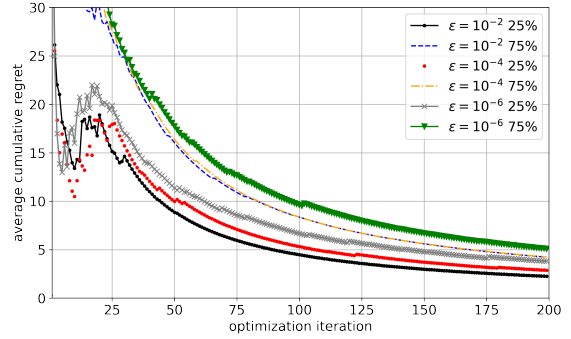
$$f(\mathbf{x}) = - \sum_{i=1}^2 \sin(x_i) \sin^{20} \left(\frac{i x_i^2}{\pi} \right) \quad (118)$$
$$\mathbf{x} \in [0, \pi]^2.$$

The optimal objective function value is -1.8013 .

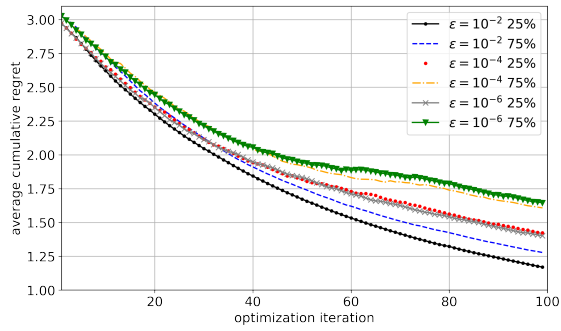
The 25th and 75th percentile of the 100 repeated runs are shown in the following figure.



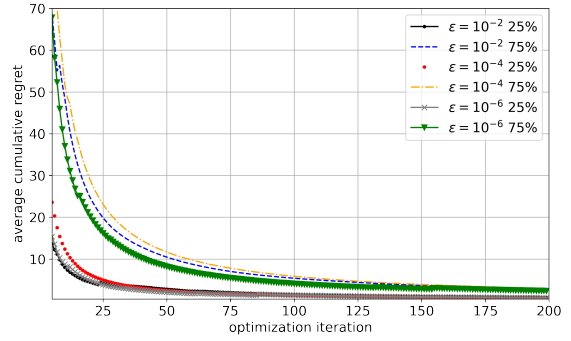
(a) Example 1: Rosenbrock function



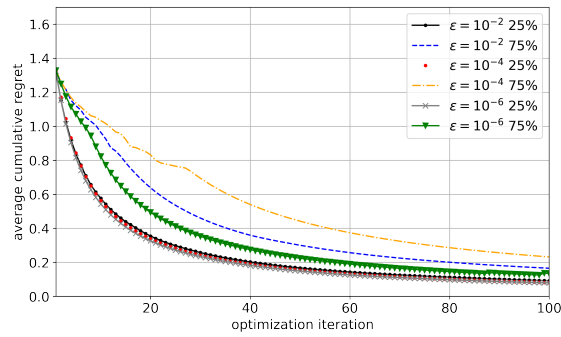
(b) Example 2: Six-hump camel function



(c) Example 3: Hartmann6



(d) Example 4: Branin function



(e) Example 5: Michalewicz function

Figure 6: 25th and 75th percentile average cumulative regret for practical EGO with nugget values 10^{-2} , 10^{-4} , and 10^{-6} for five examples.

References

- [1] S. Agrawal and N. Goyal. Analysis of thompson sampling for the multi-armed bandit problem. In *Conference on learning theory*, pages 39–1. JMLR Workshop and Conference Proceedings, 2012.
- [2] I. Andrianakis and P. G. Challenor. The effect of the nugget on gaussian process emulators of computer models. *Computational Statistics & Data Analysis*, 56(12):4215–4228, 2012.
- [3] M. Balandat, B. Karrer, D. R. Jiang, S. Daulton, B. Letham, A. G. Wilson, and E. Bakshy. BoTorch: A Framework for Efficient Monte-Carlo Bayesian Optimization. In *Advances in Neural Information Processing Systems 33*, 2020.
- [4] E. Bingham, J. P. Chen, M. Jankowiak, F. Obermeyer, N. Pradhan, T. Karaletsos, R. Singh, P. Szerlip, P. Horsfall, and N. D. Goodman. Pyro: Deep Universal Probabilistic Programming. *Journal of Machine Learning Research*, 2018.
- [5] R. Bostanabad, T. Kearney, S. Tao, D. W. Apley, and W. Chen. Leveraging the nugget parameter for efficient gaussian process modeling. *International journal for numerical methods in engineering*, 114(5): 501–516, 2018.
- [6] D. Bouneffouf, I. Rish, and C. Aggarwal. Survey on applications of multi-armed and contextual bandits. In *2020 IEEE congress on evolutionary computation (CEC)*, pages 1–8. IEEE, 2020.
- [7] A. D. Bull. Convergence rates of efficient global optimization algorithms. *Journal of Machine Learning Research*, 12(10), 2011.
- [8] R. Calandra, A. Seyfarth, J. Peters, and M. P. Deisenroth. Bayesian optimization for learning gaits under uncertainty. *Annals of Mathematics and Artificial Intelligence*, 76:5–23, February 2016.
- [9] S. R. Chowdhury and A. Gopalan. On kernelized multi-armed bandits. In *International Conference on Machine Learning*, pages 844–853. PMLR, 2017.
- [10] T. M. Cover. *Elements of information theory*. John Wiley & Sons, 1999.
- [11] P. I. Frazier. Bayesian optimization. In *Recent advances in optimization and modeling of contemporary problems*, pages 255–278, October 2018.
- [12] J. Gardner, G. Pleiss, K. Q. Weinberger, D. Bindel, and A. G. Wilson. Gpytorch: Blackbox matrix-matrix gaussian process inference with gpu acceleration. *Advances in neural information processing systems*, 31, 2018.
- [13] J. R. Gardner, M. J. Kusner, Z. Xu, K. Q. Weinberger, and J. P. Cunningham. Bayesian optimization with inequality constraints. In *Proceedings of the 31st International Conference on International Conference on Machine Learning - Volume 32*, ICML’14, pages II–937–II–945. JMLR.org, 2014.
- [14] P. E. Gill and W. Murray. Newton-type methods for unconstrained and linearly constrained optimization. *Mathematical Programming*, 7:311–350, 1974.
- [15] P. E. Gill, W. Murray, and M. H. Wright. *Practical optimization*. SIAM, 2019.
- [16] J. Gondzio. Matrix-free interior point method. *Computational Optimization and Applications*, 51: 457–480, 2012.
- [17] R. B. Gramacy and H. KH. Lee. Cases for the nugget in modeling computer experiments. *Statistics and Computing*, 22:713–722, 2012.
- [18] Nicholas J Higham. *Accuracy and stability of numerical algorithms*. SIAM, 2002.
- [19] S. Hu, H. Wang, Z. Dai, B. K. Hsiang Low, and S. H. Ng. Adjusted expected improvement for cumulative regret minimization in noisy bayesian optimization. *Journal of Machine Learning Research*, 26(46):1–33, 2025.

- [20] Shogo Iwazaki. Improved regret bounds for gaussian process upper confidence bound in bayesian optimization. *arXiv preprint arXiv:2506.01393*, 2025.
- [21] S. Jeong and S. Obayashi. Efficient global optimization (EGO) for multi-objective problem and data mining. In *2005 IEEE congress on evolutionary computation*, volume 3, pages 2138–2145. IEEE, 2005.
- [22] D. R. Jones. A taxonomy of global optimization methods based on response surfaces. *Journal of global optimization*, 21:345–383, 2001.
- [23] D. R. Jones, M. Schonlau, and W. J. Welch. Efficient global optimization of expensive black-box functions. *Journal of Global optimization*, 13:455–492, 1998.
- [24] A. Kiełbasiński. A note on rounding-error analysis of cholesky factorization. *Linear Algebra and its applications*, 88:487–494, 1987.
- [25] T. L. Lai and H. Robbins. Asymptotically efficient adaptive allocation rules. *Advances in applied mathematics*, 6(1):4–22, 1985.
- [26] D. J. Lizotte. *Practical Bayesian optimization*. PhD thesis, University of Alberta, Edmonton, Alberta, Canada, 2008.
- [27] C. J. Lourenco and E. Moreno-Centeno. Exactly solving sparse rational linear systems via roundoff-error-free Cholesky factorizations. *SIAM Journal on Matrix Analysis and Applications*, 43(1):439–463, 2022.
- [28] Y. Lyu, Y. Yuan, and I. W. Tsang. Efficient batch black-box optimization with deterministic regret bounds. *arXiv preprint arXiv:1905.10041*, 2019.
- [29] R. Martinez-Cantin. Bayesopt: A Bayesian optimization library for nonlinear optimization, experimental design and bandits. Technical report, 2014.
- [30] J. Meinguet. Refined error analyses of cholesky factorization. *SIAM journal on numerical analysis*, 20(6):1243–1250, 1983.
- [31] M. Molga and C. Smutnicki. Test functions for optimization needs. *Test functions for optimization needs*, 101(48):32, 2005.
- [32] V. Nguyen, S. Gupta, S. Rana, C. Li, and S. Venkatesh. Regret for expected improvement over the best-observed value and stopping condition. In *Proceedings of the Ninth Asian Conference on Machine Learning*, volume 77, pages 279–294. PMLR, 2017.
- [33] F. Pedregosa, G. Varoquaux, A. Gramfort, V. Michel, B. Thirion, O. Grisel, M. Blondel, P. Prettenhofer, R. Weiss, V. Dubourg, J. Vanderplas, A. Passos, D. Cournapeau, M. Brucher, M. Perrot, and E. Duchesnay. Scikit-learn: Machine learning in Python. *Journal of Machine Learning Research*, 12:2825–2830, 2011.
- [34] A. Pepelyshev. The role of the nugget term in the gaussian process method. In *mODa 9—Advances in Model-Oriented Design and Analysis: Proceedings of the 9th International Workshop in Model-Oriented Design and Analysis held in Bertinoro, Italy, June 14–18, 2010*, pages 149–156. Springer, 2010.
- [35] V. Picheny, T. Wagner, and D. Ginsbourger. A benchmark of kriging-based infill criteria for noisy optimization. *Structural and multidisciplinary optimization*, 48:607–626, 2013.
- [36] H. Robbins. Some aspects of the sequential design of experiments. *Bulletin of the American Mathematical Society*, 1952.
- [37] I. O. Ryzhov. On the convergence rates of expected improvement methods. *Operations Research*, 64(6): 1515–1528, 2016.

- [38] P. Saves, R. Lafage, N. Bartoli, Y. Diouane, J. Bussemaker, T. Lefebvre, J. T. Hwang, J. Morlier, and J. R. R. A. Martins. SMT 2.0: A surrogate modeling toolbox with a focus on hierarchical and mixed variables gaussian processes. *Advances in Engineering Software*, 188:103571, 2024. doi: <https://doi.org/10.1016/j.advengsoft.2023.103571>.
- [39] R. B. Schnabel and E. Eskow. A new modified cholesky factorization. *SIAM Journal on Scientific and Statistical Computing*, 11(6):1136–1158, 1990.
- [40] M. Schonlau, W. J. Welch, and D. R. Jones. Global versus local search in constrained optimization of computer models. *Lecture notes-monograph series*, pages 11–25, 1998.
- [41] N. Srinivas, A. Krause, S. M. Kakade, and M. Seeger. Gaussian process optimization in the bandit setting: No regret and experimental design. *arXiv preprint arXiv:0912.3995*, 2009.
- [42] J. Sun. Componentwise perturbation bounds for some matrix decompositions. *BIT Numerical Mathematics*, 32(4):702–714, 1992.
- [43] The GPyOpt authors. Gpyopt: A bayesian optimization framework in python. <http://github.com/SheffieldML/GPyOpt>, 2016.
- [44] H. Tran-The, S. Gupta, S. Rana, and S. Venkatesh. Regret bounds for expected improvement algorithms in gaussian process bandit optimization. *arXiv preprint arXiv:2203.07875*, 2022.
- [45] S. Vakili. Open problem: Regret bounds for noise-free kernel-based bandits. In *Conference on Learning Theory*, pages 5624–5629. PMLR, 2022.
- [46] S. Vakili, K. Khezeli, and V. Picheny. On information gain and regret bounds in Gaussian process bandits. In *International Conference on Artificial Intelligence and Statistics*, pages 82–90. PMLR, 2021.
- [47] F. AC. Viana, R. T. Haftka, and L. T. Watson. Efficient global optimization algorithm assisted by multiple surrogate techniques. *Journal of Global Optimization*, 56:669–689, 2013.
- [48] K. Wang, G. Pleiss, J. Gardner, S. Tyree, K. Q. Weinberger, and A. G. Wilson. Exact gaussian processes on a million data points. *Advances in neural information processing systems*, 32, 2019.
- [49] X. Wang, Y. Jin, S. Schmitt, and M. Olhofer. Recent advances in Bayesian optimization. *ACM Comput. Surv.*, 55(13s), jul 2023.
- [50] Z. Wang and N. de Freitas. Theoretical analysis of bayesian optimisation with unknown gaussian process hyper-parameters, 2014. URL <https://arxiv.org/abs/1406.7758>.
- [51] J. H. Wilkinson. A priori error analysis of algebraic processes. In *Intern. Congress Math*, volume 19, pages 629–639, 1968.
- [52] S. J. Wright. Modified cholesky factorizations in interior-point algorithms for linear programming. *SIAM Journal on Optimization*, 9(4):1159–1191, 1999.
- [53] J. Wu, X. Chen, H. Zhang, L. Xiong, H. Lei, and S. Deng. Hyperparameter optimization for machine learning models based on bayesian optimization. *Journal of Electronic Science and Technology*, 17(1): 26–40, 2019.
- [54] M. Zaefferer, J. Stork, M. Friese, A. Fischbach, B. Naujoks, and T. Bartz-Beielstein. Efficient global optimization for combinatorial problems. In *Proceedings of the 2014 Annual Conference on Genetic and Evolutionary Computation, GECCO '14*, page 871–878, New York, NY, USA, 2014. Association for Computing Machinery.